

INFORMATION TO USERS

The most advanced technology has been used to photograph and reproduce this manuscript from the microfilm master. UMI films the text directly from the original or copy submitted. Thus, some thesis and dissertation copies are in typewriter face, while others may be from any type of computer printer.

The quality of this reproduction is dependent upon the quality of the copy submitted. Broken or indistinct print, colored or poor quality illustrations and photographs, print bleedthrough, substandard margins, and improper alignment can adversely affect reproduction.

In the unlikely event that the author did not send UMI a complete manuscript and there are missing pages, these will be noted. Also, if unauthorized copyright material had to be removed, a note will indicate the deletion.

Oversize materials (e.g., maps, drawings, charts) are reproduced by sectioning the original, beginning at the upper left-hand corner and continuing from left to right in equal sections with small overlaps. Each original is also photographed in one exposure and is included in reduced form at the back of the book. These are also available as one exposure on a standard 35mm slide or as a 17" x 23" black and white photographic print for an additional charge.

Photographs included in the original manuscript have been reproduced xerographically in this copy. Higher quality 6" x 9" black and white photographic prints are available for any photographs or illustrations appearing in this copy for an additional charge. Contact UMI directly to order.

U·M·I

University Microfilms International
A Bell & Howell Information Company
300 North Zeeb Road, Ann Arbor, MI 48106-1346 USA
313/761-4700 800/521-0600

Order Number 9017191

Nitrogen flux in the northern Bering Sea

Hansell, Dennis Arthur, Ph.D.

University of Alaska Fairbanks, 1989

U·M·I
300 N. Zeeb Rd.
Ann Arbor, MI 48106

NITROGEN FLUX IN THE NORTHERN BERING SEA

A
THESIS

Presented to the Faculty of the University of Alaska
in Partial Fulfillment of the Requirements
for the Degree of

DOCTOR OF PHILOSOPHY

By

Dennis Arthur Hansell, B.A., M.S.

Fairbanks, Alaska

May 1989

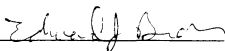
NITROGEN FLUX IN THE NORTHERN

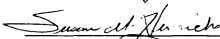
BERING SEA

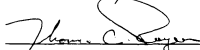
by


Dennis Arthur Hansell


RECOMMENDED








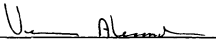


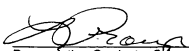


Advisory Committee Chair


Department Head

APPROVED



Dean, School of Fisheries and Ocean
Sciences


Dean of the Graduate School

5/1/89

Date

ABSTRACT

Much of the primary production occurring over the Bering Sea continental shelf is thought to be associated with both ice edge and spring blooms. The nature of summer production over the shelf is now being addressed. A general model is presented for summer phytoplankton production along the Bering Sea shelf break front and subsequent transport of phytodetritus into the northern Bering Sea. Production associated with the shelf break front is estimated to be $200 \text{ g} \cdot \text{C} \cdot \text{m}^{-2}$ over a 120-day growing season and is supported by nutrients from the Bering Slope Current. A portion of the biomass accumulating over the front is advected into the Chirikov Basin, supplying 26% of the daily carbon demand of the benthos.

The Bering Slope Current bifurcates at Cape Navarin and one branch, referred to as the Anadyr Current, flows north through Anadyr and Bering Straits. Nutrients in the Anadyr Current support an intense surface bloom over the western Chirikov Basin where total nitrogen uptake rates are $>6.0 \text{ mg-at N} \cdot \text{m}^{-2} \cdot \text{h}^{-1}$ and nitrate contributes up to 50% of the total nitrogen uptake. Modified Bering Shelf water contains phytoplankton at two depths: both a surface accumulation and a deep layer. Nitrate contributes $<35\%$ to total nitrogen uptake rates of $1.80 \text{ mg-at N} \cdot \text{m}^{-2} \cdot \text{h}^{-1}$ in this water. Nitrogen productivity is lowest in Alaskan Coastal water ($1.0 \text{ mg-at N} \cdot \text{m}^{-2} \cdot \text{h}^{-1}$) where nitrate uptake averages only 15% of the total. A simple nitrogen budget suggests that 29% and 62% of the annual nitrogen productivity in modified Bering Shelf and Anadyr waters, respectively, is exported through Bering Strait into the southern Chukchi Sea for deposition.

Improved estimates of the rates of urea production and uptake by phytoplankton in the northern Bering Sea were made after determining the change in ^{15}N -atom % enrichment of urea during incubations. Estimates of uptake rates increased by up to

83% using a ^{15}N accumulation model and by >210% using a ^{15}N disappearance model. However, a discrepancy exists between the ^{15}N -urea removed from the aqueous phase and the ^{15}N accumulated in the particulate phase. The ability to find in the particulate fraction the ^{15}N removed from solution as ^{15}N -urea was improved by 72% following removal of the >20- μm particulate fraction.

TABLE OF CONTENTS

ABSTRACT	iii
TABLE OF CONTENTS.....	v
LIST OF FIGURES	vii
LIST OF TABLES	ix
ACKNOWLEDGEMENTS	x
INTRODUCTION: NITROGEN FLUX IN THE NORTHERN BERING SEA.....	1
CHAPTER 1. SUMMER PHYTOPLANKTON PRODUCTION AND TRANSPORT ALONG THE SHELF BREAK IN THE BERING SEA	-
INTRODUCTION	5
METHODS	7
RESULTS AND DISCUSSION	
General hydrography of the Bering Sea shelf and slope.....	8
Shelf break chlorophyll distribution and transport	11
Transit through Anadyr and Shpanberg Straits.....	18
Deposition and regeneration in the northern Bering Sea	25
Production at the shelf break front	26
Surface blooms in the ISHTAR area	
East bloom	26
West bloom.....	28
SUMMARY	
General model for summer production and consumption on the northern Bering Sea shelf.....	32

CHAPTER 2. PELAGIC NITROGEN FLUX IN THE NORTHERN BERING SEA	
INTRODUCTION	3 6
METHODS	3 6
RESULTS AND DISCUSSION.....	3 8
Anadyr water and the west bloom.....	4 1
Modified Bering Shelf water, deep chlorophyll, and the east bloom.....	4 6
Alaskan Coastal water.....	5 1
Contribution of regenerated nutrients.....	5 1
Estimation of nitrogen productivity in shelf water.....	5 3
Export of shelf water detritus to the southern Chukchi Sea.....	5 6
CHAPTER 3. A METHOD FOR ESTIMATING UPTAKE AND PRODUCTION	
RATES FOR UREA IN SEAWATER USING ¹⁴ C- AND ¹⁵ N-UREA	
INTRODUCTION	6 1
The Dual-Label Model.....	6 3
METHODS	6 5
RESULTS AND DISCUSSION.....	6 6
CHAPTER 4. SUMMARY AND CONCLUSIONS	7 4
REFERENCES	8 3

LIST OF FIGURES

Figure 1.1	A portion of the Bering-Chukchi shelf.....	6
Figure 1.2	The cross shelf advection/diffusion model developed by the PROBES investigators.....	9
Figure 1.3	Locations of hydrographic fronts on the Bering Sea shelf.....	10
Figure 1.4	Distribution of chlorophyll <i>a</i> over the southeastern Bering Sea shelf.....	12
Figure 1.5	Locations of transects.....	13
Figure 1.6	Vertical cross-sections from Transect A.....	14
Figure 1.7	Vertical cross-sections from Transect F.....	16
Figure 1.8	Areal distribution of chlorophyll <i>a</i> along Transect A.....	17
Figure 1.9	Vertical cross-sections from Transect B.....	19
Figure 1.10	Vertical cross-sections from Transect C.....	20
Figure 1.11	Vertical cross-sections from Transect D.....	21
Figure 1.12	Distribution of bottom salinity in July 1987.....	22
Figure 1.13	Distribution of chlorophyll integrated from 15 m to the bottom.....	23
Figure 1.14	Vertical cross-sections of chlorophyll <i>a</i> in Anadyr and Shpanberg Straits.....	24
Figure 1.15	Vertical cross-sections from Transect E.....	27
Figure 1.16	Distribution of chlorophyll integrated from the surface to 15 m.....	29
Figure 1.17	Vertical cross-sections from Transect G.....	30
Figure 1.18	Generalized model for the production and transport of plant biomass.....	33

Figure 1.19	Diagrammatic latitudinal cross-section depicting relative positions of the water masses.....	3 5
Figure 2.1a	Locations of stations occupied during TT 213.....	3 9
Figure 2.1b	Locations of stations occupied during TT 214.....	4 0
Figure 2.2	Distribution of integrated nitrate during TT 213.....	4 2
Figure 2.3	Distribution of integrated chlorophyll during TT 213.....	4 3
Figure 2.4	Depth distribution of salinity, total nitrogen specific uptake rates, particulate nitrogen and nitrate for productivity Station 97.....	4 7
Figure 2.5	Depth distribution of salinity, total nitrogen specific uptake rates, particulate nitrogen and nitrate for productivity Station 39.....	4 8
Figure 2.6	Depth distribution of salinity, total nitrogen specific uptake rates, particulate nitrogen and nitrate for productivity Station 13.....	5 0
Figure 2.7	Depth distribution of salinity, total nitrogen specific uptake rates, particulate nitrogen and nitrate for productivity Station 111.....	5 2
Figure 2.8	Mean depth and mean total nitrogen specific uptake rates for seven photosynthetically active radiation depths.....	5 4
Figure 2.9	An annual nitrogen budget.....	5 8

LIST OF TABLES

	PAGE
Table 2.1 The range and mean of total nitrogen productivity.....	4 5
Table 3.1 Absolute uptake rate of urea	6 7
Table 3.2 Fraction of ¹⁵ N-urea removed from the dissolved phase.....	6 9

ACKNOWLEDGEMENTS

This dissertation is the result of 4 years of effort at the Institute of Marine Science. My stay at the Institute has been pleasurable and rewarding and I will always remember those students, faculty, and staff who have made it so. The Institute has been under the leadership of Vera Alexander during my tenure and she deserves credit for providing a stimulating working environment.

The project of which I have been a member since 1985 (ISHTAR) was funded by the National Science Foundation's Division of Polar Programs (DPP 84-05286). I believe that the project has resulted in a timely and important understanding of the ecosystem in the Bering Strait region and I thank the Division for their support. The scientists making up the ISHTAR party (an appropriate term given our visits to Nome) have been essential to development of this dissertation. My work could not have been completed without the great quantity of supporting data that all involved had a hand in collecting. We bounced a few good ideas (and maybe one or two bad ones) off of each other and I think that we have come up with sound concepts about how the ecosystem works. I thank them for their support and friendship.

Members of my graduate advisory committee have been very supportive. They gave me the leeway to pursue the work as I deemed appropriate while maintaining an active interest in my progress. I was told that the committee left me to my own devices because I had their trust. I valued that trust. Members of the committee are: Bill Reeburgh, Susan Henrichs, Tom Royer and Ed Brown. I thank them for their friendship and guidance.

John Goering has been my advisor since the beginning. We met in the fall of 1984 when I was returning to school after having been out of the academic mill for a few years. I remember being given the ISHTAR proposal and being told to be ready for a July cruise. Having never before worked on a ship or in oceanography I was apprehensive

about my potential for success. John must have thought otherwise because for four years he gave me complete freedom - and, to paraphrase Gandhi, 'complete freedom includes the freedom to err.' And I had my 'share of err.' I hope that should I have the opportunity to advise students I will allow them to learn with a similar freedom. John has been my friend and I will always value what I have learned from him.

My parents, brothers and sisters are some of my favorite people. I wish to acknowledge them by name because they are important to me: Paul and Rose Marie, my parents; and my siblings, in descending order of age: Bernadette, Michael, Peter, Mary Jo, Thomas, and Susan. I love you all very much!

Most importantly, I thank my best friend Paula. I have no more important a supporter than she. Paula helped me through the tough times when my confidence had waned and I'm sure she'll be doing it again. She is an "awesome" spouse and mother and I love her dearly (this should get me those brownies I've been after). I would not have undertaken this effort if not for her. Thank you, Paula.

This dissertation is dedicated to our children. We wish them all the happiness that life has brought to us. You are limited only by your imagination.

INTRODUCTION: NITROGEN FLUX IN THE NORTHERN BERING SEA

Nitrogen in the marine environment takes many forms and plays many roles. As such, marine scientists have long used the element to trace biological, chemical, and physical oceanographic processes occurring over a broad range of temporal and spatial scales. The element is particularly appealing to biologists and chemists interested in the cycling of biologically important elements. Nitrogen is a component of both inorganic and organic compounds in seawater, the latter taking dissolved and particulate forms (Sharp, 1983). In its inorganic and dissolved organic forms nitrogen often serves as the growth-limiting nutrient to phototrophs and bacteria (Dugdale and Goering, 1967; Paul, 1983; Wheeler and Kirchman, 1986) while serving as an excretory product to heterotrophs (Bidigare, 1983). In this dissertation, nitrogen, in several of its forms, is cast as the unifying character in describing and quantifying some of the biological and physical processes occurring over the northern Bering Sea shelf in summer.

The northern Bering and southern Chukchi Seas have been the subject of extensive oceanographic surveys since 1985 as part of the Inner Shelf Transfer and Recycling (ISHTAR) program. The program was designed to assess the fate of the dissolved and particulate phases of carbon, nitrogen, phosphorus, and silicon in the northern Bering and southern Chukchi Seas (Walsh *et al.*, in press). A primary motivation for this effort was the desire to understand the processes sustaining the rich ecosystem known to exist in this subpolar region. Field studies conducted over the past few decades have resulted in a nearly comprehensive understanding of the regional physical oceanography (Coachman *et al.*, 1975). A survey of primary productivity in the area (Sambrotto *et al.*, 1984) provided an initial estimate of the potential magnitude of primary productivity but an incomplete explanation for the processes controlling it.

Early in the ISHTAR program, regions exhibiting major phytoplankton blooms were mapped, and rates of primary production quantified, in the northern Bering and southern Chukchi

Seas (Springer, 1988). These highly productive areas were assumed to be the major sources of organic carbon and nitrogen necessary to support the rich higher-trophic populations known to thrive in the Chirikov basin, of the northern Bering Sea, and in the southern Chukchi Sea (Stoker, 1981; Grebmeier, 1987; Springer, 1988). However, the accepted paradigm for the production and fate of organic matter did not, in my view, survive close scrutiny. For instance, a spatial discrepancy existed between the location of the major bloom in the northern Bering Sea and the location of maximum benthic biomass in the same region. The most concentrated benthic biomass was located 20-30 kilometers to the east and south of the major phytoplankton bloom. It did not appear physically possible, in this strong northerly advective system, to deposit organic carbon and nitrogen such a distance to the east of the bloom. Allochthonous sources of organic matter had to be invoked to support the benthic food web. It was clear that we had not fully elucidated the sources and fate of particulate organic nitrogen and carbon over the northern Bering Sea shelf.

Earlier studies of the southeastern Bering Sea shelf (PROBES) resulted in models of the general circulation (Coachman, 1986) and primary productivity patterns (Sambrotto *et al.*, 1986) upstream of the ISHTAR study area. In concert with these results, I address the following questions in Chapters 1 and 2: What is the geographical distribution of primary productivity over the entire Bering Sea shelf and can this distribution be integrated with existing models for primary productivity over the southeastern shelf?; What are the physical processes that give form and dimension to the productivity system?; What are the rates of nitrogen productivity in the water masses endemic to the northern Bering Sea?; What is the fate (geographical and trophic level) of the nitrogen-based primary productivity on an annual basis? To aid in answering these questions, hydrographic, nutrient, and chlorophyll data were taken from ISHTAR Data Reports No. 1 (1985) and No. 9 (1987).

As mentioned above, nitrogen can be found in inorganic and organic forms and both forms may be used by phytoplankton to meet their nutritive requirements and by heterotrophs as excretory products. Determining the rate of autotrophic assimilation and heterotrophic production of specific nitrogen compounds can be a difficult task, though. The nitrogen isotope ^{15}N has proved especially useful in determining rates of uptake of nitrogen-containing compounds such as nitrate and ammonium since Dugdale and Goering (1967) first introduced the method.

The nitrogen cycle in the northern Bering Sea includes one component not currently recognized as important in the open ocean. That component is the nitrogen-rich molecule urea. Urea is produced by zooplankton as a nontoxic excretory product and by bacteria in the degradation of purines and pyrimidines (Bidigare, 1983; Gottschalk, 1986). Once urea is released to the water column, it becomes available to phytoplankton as a nitrogen source (McCarthy, 1972). After assimilation of the compound by a plant cell, an energy-dependent enzymatic step is necessary to split the urea molecule into two ammonium ions and CO_2 (Paul, 1983). Because incorporation of urea nitrogen is energy dependent, ammonium is the substrate preferred by phytoplankton to meet their nutritional needs. However, in nutrient-impovertished waters, phytoplankton will utilize urea fully. Such is the case in the two nutrient-deficient water masses of the northern Bering Sea.

Development of a method to directly measure both uptake and production of urea has proved elusive. To achieve an accurate measure of the uptake rate of a regenerated nutrient such as urea, the change in enrichment of the labeled nutrient must be determined over the course of an incubation. Determining this change, along with the change in concentration of the nutrient, provides for estimates of the rates of uptake and production of the nutrient after correction for isotope dilution (Gilbert *et al.*, 1982). In determining uptake and production rates for ammonium, another regenerated nutrient, the ion must be removed from solution to determine its

^{15}N -enrichment by spectrometry. Several methods have been used for this purpose (Glibert *et al.*, 1982; Fisher and Morrissey, 1985; Dudek *et al.*, 1986; Lipshultz *et al.*, 1986; Selmer and Sorensson, 1986). Significantly, methods do not exist for the removal from solution, and mass spectrometric analysis, of the urea pool.

Fortunately, urea is composed of both carbon and nitrogen atoms. In nitrogen uptake experiments, the goal is to measure the accumulation of ^{15}N in the particulate fraction. To correct for isotope dilution, one must know the initial and final concentrations of ^{15}N -labeled urea in solution. By labeling urea with ^{15}N , we have a means of measuring the accumulation of urea-N in the particulate fraction. Further, by labeling urea with ^{14}C , we have a mechanism for measuring the amount of ^{15}N -urea remaining in solution. Given these two values, a more accurate determination of the uptake and production rates of urea can be made. The objective of Chapter 3 is to describe such a method.

As a whole, this thesis examines the distribution, transport, and consumption of primary productivity over the Bering Sea shelf in summer using the biological uptake of nitrate, ammonium, and urea to identify and quantify these important processes. Because of its central role in elemental cycling nitrogen is an important tool for tracing physical, chemical, and biological processes, thus providing a better understanding of this highly productive ecosystem.

CHAPTER 1: SUMMER PHYTOPLANKTON PRODUCTION AND TRANSPORT ALONG THE SHELF BREAK IN THE BERING SEA

INTRODUCTION

Our understanding of the magnitude, location, and fate of primary production in the vicinity of the Bering Sea continental shelf is increasing rapidly. Results from recent and ongoing studies in the region suggest that contributions to annual production on the shelf include: production due to epontic ice algae (McRoy and Goering, 1974); spring ice-edge blooms (Niebauer and Alexander, 1985), which follow the receding ice-edge from deep water onto the shelf; spring blooms over the shelf, which are maintained into the summer by occasional wind mixing events (Sambrotto *et al.*, 1986); spring blooms at the shelf break front (Iverson *et al.*, 1979a); and summer production on the northeastern shelf (Springer, 1988).

I hypothesize that summer production along the shelf break front (the interface between distinct water masses) contributes significantly to total shelf production. A general model is presented for summer phytoplankton production and transport along the Bering Sea shelf break front into the northern Bering and southern Chukchi Seas. I suggest that the nutrients of the Bering Slope Current support two regions of primary productivity in the Bering Sea throughout the summer: along the shelf break front and in the western portion of the Chirikov Basin (Fig. 1.1).

First, cumulative evidence (recently collected and historical data) suggests that plant production takes place above the shelf break front in the spring and summer. Iverson *et al.* (1979b) noted that the spring chlorophyll maximum found over the shelf break front in the southeastern Bering Sea persisted for about one month, slowly sinking at a rate of about 1 m d^{-1} . In this chapter I propose that the biomass (in excess of loss due to grazing) accumulates along the front at the pycnocline and is transported with the slope current to the northwest toward Cape

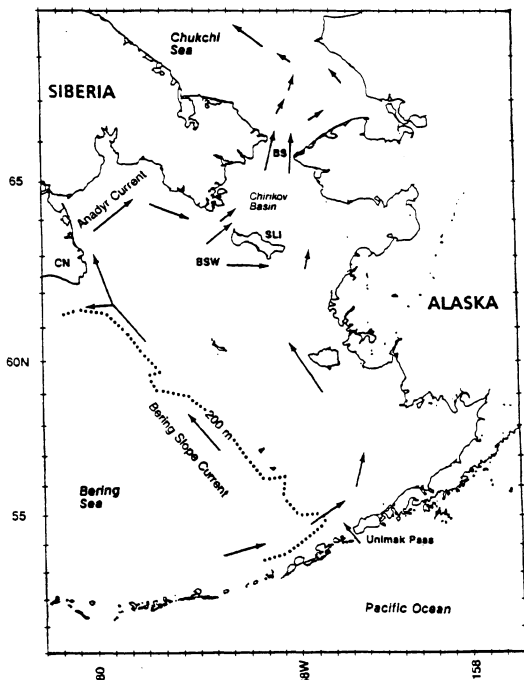


Figure 1.1 A portion of the Bering-Chukchi shelf, with generalized circulation patterns. The ISHTAR study area lies north of St. Lawrence Island (SLI) and south of 69° N. Bering Strait (BS) and modified Bering Shelf water (BSW) are indicated. Anadyr Strait is located between Siberia and St. Lawrence Island and Shpanberg Strait is located between St. Lawrence Island and the Alaskan mainland. Arrows do not represent relative magnitude of current speed. Mean current speeds in Bering, Anadyr, and Shpanberg Straits are 25, 15, and 5 cm s^{-1} (Aagaard *et al.*, 1985).

Navarin, across the Gulf of Anadyr, and through Anadyr and Shpanberg Straits. This production and transport process is analogous to a continuous culture system where, as the plants are transported and grazed, a ready supply of nutrients maintain the plants at high levels.

Malone *et al.* (1983) described a similar production and transport process at the shelf break of the New York Bight. They found that development of stratification in nutrient-rich offshore water between storm events results in high growth rates and biomass near the surface on the shelf side of the shelf break front. During the summer, and as is the case at the Bering Sea shelf break, plant growth occurred at the pycnocline. Unlike the Bering Sea, however, where transport is from the shelf break front to the inner shelf, up to 35% of annual production over the continental shelf of the New York Bight is exported from shelf to slope water.

The second important region of summer production is associated with the western boundary current (the northern extension of the Bering Slope Current known as the Anadyr Current) south of Bering Strait. Nutrients carried by the Anadyr Current support intense surface production following passage through Anadyr Strait. Biomass produced in this region is transported north through Bering Strait for deposit in the southern Chukchi Sea.

METHODS

Data were collected during cruises on the R/V *Alpha Helix* (July 1985 and October 1987) and the R/V *T. G. Thompson* (July - August 1987) as part of the Inner Shelf Transfer and Recycling (ISHTAR) project. The study area included the region around St. Lawrence Island in the south to approximately 69° N latitude and from the Alaskan coast in the east to the United States - Soviet 1867 Convention Line in the west. The methods used for determination of the water column conductivity and temperature, chlorophyll *a* and nutrient concentrations, and particulate nitrogen (PN) concentrations are described in Chapter 2.

RESULTS AND DISCUSSION

General Hydrography of the Bering Sea Shelf and Slope

The Bering Sea is broadly divided into two regions: the deep Aleutian Basin (>3500 m depth), which accounts for 40% of the area of the Bering Sea; and the continental shelf region (<200 m depth), accounting for another 40%. These regions are divided by an approximately 1000 km long shelf break, which has its origins in the southeast near Unimak Pass, Alaska, and in the northwest near Cape Navarin, Soviet Union (Fig. 1.1).

A strong shelf break front is a persistent feature over the shelf slope (Fig. 1.2). It separates oceanic water (>32.7 ppt) in the Aleutian Basin from 31.0-32.7 ppt shelf water. The geostrophic Bering Slope Current is found on the basin side of the shelf break front and has an estimated transport of 5 Sv (1 Sv is equivalent to $10^6 \text{ m}^3 \cdot \text{s}^{-1}$) and a speed of up to $10 \text{ cm} \cdot \text{s}^{-1}$. Long-term mean flow on the shelf side of the front is estimated to be $5 \text{ cm} \cdot \text{s}^{-1}$ (Coachman, 1986).

Shelf water is divided into domains by fronts (Fig. 1.2) that are closely aligned with specific isobaths (Coachman, 1986). To the east is Alaskan Coastal water (<31.0 ppt), which is a mixture of deep Bering Sea water advected onto the shelf near Unimak Pass and fresh river water (Kinder and Coachman, 1978). An inner front, found at the 50 m isobath, separates the coastal water from the slowly moving ($1 \text{ cm} \cdot \text{s}^{-1}$) middle domain. A strongly stratified two-layered system, the middle domain is separated from the outer domain by the middle front located near the 100 m isobath. Finally, the outer domain is separated from the Bering Slope Current by the shelf break front.

The inner front can be traced to the northwest along the 50 m isobath. At a point south of Shpanberg Strait, the front leaves the 50 m isobath, deviating to the north through Shpanberg and Bering Straits (Fig. 1.3). The identity of the middle front is lost south of St. Lawrence Island, whereas the shelf break front can be traced to a point near Cape Navarin where it deviates from the 200 m isobath, turning north toward Anadyr and Bering Straits (Coachman, 1986). The upper

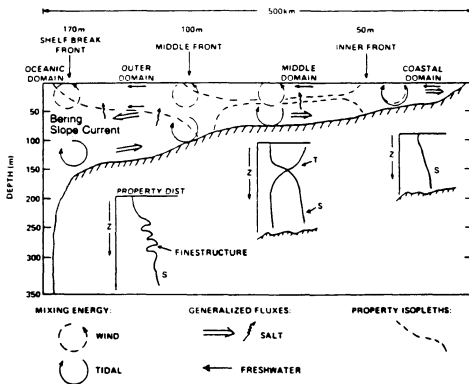


Figure 1.2 The cross shelf advection/diffusion model developed by PROBES investigators which relates the vertical energy distributions to the typical horizontal and vertical property distributions and the fronts, and the inferred freshwater and salt fluxes (from Coachman *et al.*, 1980, with additions).

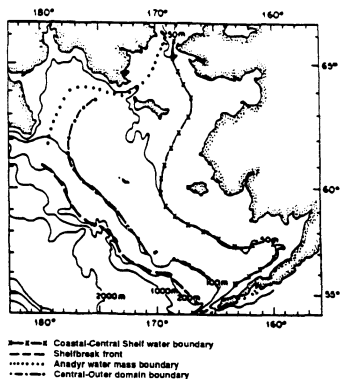


Figure 1.3 Locations of hydrographic fronts on the Bering Sea shelf (from Coachman, 1986).

layer of the Bering Slope Current bifurcates at Cape Navarin and is advected across the Gulf of Anadyr and north through Bering Strait as a separate identifiable water mass (here referred to as Anadyr water). Cumulative observational evidence supports the idea that Anadyr water flows northward across the gently shoaling eastern Bering Sea continental shelf as a western boundary current along the Siberian coast (Kinder *et al.*, 1986). Throughout summer, the northern extension of the shelf break front is located in Anadyr Strait and the inner front is found in Shpanberg Strait (Fig. 1.3). Disappearance of the middle front is the result of the merging of middle and outer domains southwest of St. Lawrence Island, resulting in a water mass referred to as modified Bering Shelf water (Shelf water). The two remaining fronts (shelf break and inner) separate the three water masses that pass through Bering Strait: Alaskan Coastal water (<31.5 ppt) to the east, modified Bering Shelf water (31.5-32.7 ppt), and Anadyr water (>32.7 ppt) to the west. Long-term average flow in summer through Bering Strait is estimated at 1.1 Sv (Coachman and Aagaard, 1988). Mean current speeds through Bering, Anadyr, and Shpanberg Straits have been estimated to be 25, 15, and 5 $\text{cm} \cdot \text{s}^{-1}$, respectively (Aagaard *et al.*, 1985).

Shelf Break Chlorophyll Distribution and Transport

The May, 1978 areal distribution of chlorophyll *a* in the southeastern Bering Sea (Fig. 1.4), demonstrates the presence of a spatially distinct accumulation of plant biomass ($100 \text{ mg} \cdot \text{m}^{-2}$) located over the shelf break (Iverson *et al.*, 1979a). Chlorophyll concentrations were < 50 $\text{mg} \cdot \text{m}^{-2}$ on both the shelf and basin sides of the shelf break accumulation and increased to 400 $\text{mg} \cdot \text{m}^{-2}$ over the middle shelf, reflecting the presence of the spring bloom (Sambrotto *et al.*, 1986).

Vertical profiles of water column characteristics along transect A (Fig. 1.5), originating in Anadyr Strait and terminating at the shelf break (July 1987), provides insight on the horizontal transport of the plant biomass that had accumulated above the shelf break front. An approximate mirror image exists for water column profiles of salinity, temperature, and nitrate and the axis of this image is broadly centered around the 75 m bottom contour (Fig. 1.6). Based on general flow

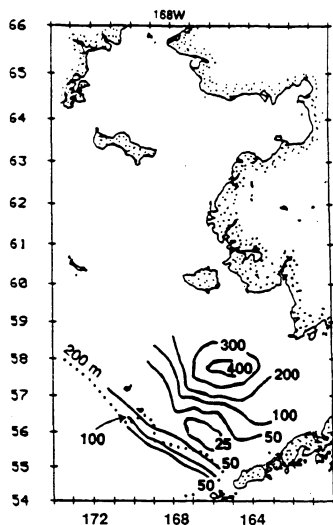


Figure 1.4 Distribution of chlorophyll *a* ($\text{mg} \cdot \text{m}^{-2}$) in the southeastern Bering Sea in May 1978 and the 200 m isobath (redrawn from Iverson *et al.*, 1979a).

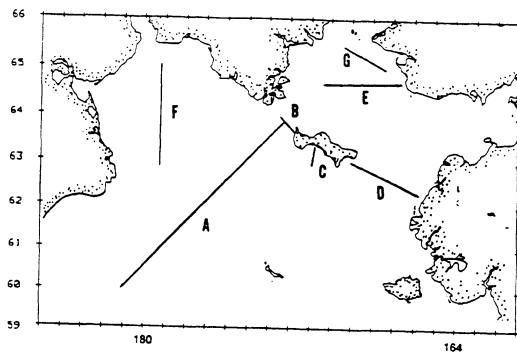


Figure 1.5 Locations of transects.

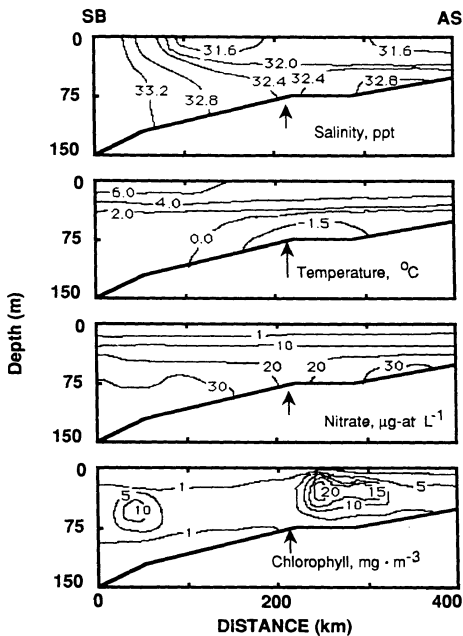


Figure 1.6 Vertical cross-section from Transect A in July 1987. Arrows indicate the approximate point about which the flow rotates on this transect. The transect originates in Anadyr Strait (AS) and terminates at the shelf break (SB).

patterns in the area (Fig. 1.1) as described by Coachman *et al.* (1975), it is apparent that the water overlying the > 75 m sea-bottom flows to the northwest toward Cape Navarin, while the water overlying the <75 m sea-bottom moves to the northeast, through Anadyr Strait, and southeast, south of St. Lawrence Island. Hence, the point on this transect (marked by an arrow in Fig. 1.6) about which the northern extension of the Bering Slope Current rotates is the 75 m depth. The very cold temperature at this point (<-1.5°C) suggests that the origin of this central pool is winter-cooled water (Coachman *et al.*, 1975) that is not easily displaced (Fig. 1.6). The northern extension of the Bering Slope Current (>32.7 ppt Anadyr water) crosses the Gulf of Anadyr and continues north through Anadyr Strait (Fig. 1.1). Chlorophyll *a* accumulation is evident above the front at the shelf break, with the maximum concentration increasing from 10 mg · m⁻³ over the shelf break to >20 mg · m⁻³ at Anadyr Strait (Fig. 1.6).

Based on salinity and nitrate distributions from transect F (Fig. 1.5), it appears that following bifurcation at Cape Navarin, the main flow of Anadyr water is located over the 70 m isobath (Fig. 1.7). The salinity profile broadly locates Shelf water above the 90 m isobath. Near the coast, in the Gulf of Anadyr, salinity is > 34.0 ppt, a value not in character with Anadyr water. It is likely that the coastal water is residual from winter as indicated by a very low near-bottom temperature (-1.6°C) and reduced nitrate concentrations (Fig. 1.7). The highest nitrate values overlie the 70 m isobath, suggesting that this isobath lies beneath the main flow line.

The areal distribution of chlorophyll south of St. Lawrence Island (Fig. 1.8) reveals that bifurcation of Shelf water occurs at the west end of St. Lawrence Island. A portion of Shelf water plant biomass enters Chirikov Basin (the region north of St. Lawrence Island and south of Bering Strait; Fig. 1.1) via Anadyr Strait, with the remainder flowing to the east, south of St. Lawrence Island. A portion of that plant and detrital material transported south of the island transits the western end of Shpanberg Strait. It is likely that a portion of the plant material transported south of St. Lawrence Island is deposited during transit.

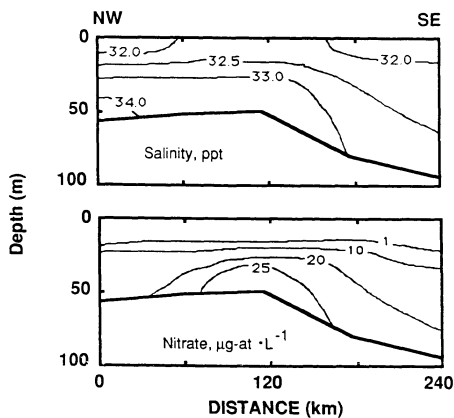


Figure 1.7 Vertical cross-sections from Transect F in August 1970 (profiles drawn from data of Husby and Hufford, 1970). The transect originates in northwestern Gulf of Anadyr (NW) and terminates to the southeast (SE).

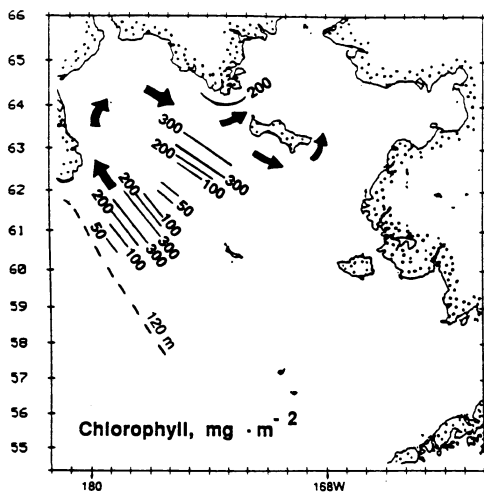


Figure 1.8 Areal distribution of chlorophyll ($\text{mg} \cdot \text{m}^{-2}$) along Transect A and presumed circulation in July 1987. Chlorophyll isolines are drawn according to presumed direction of flow.

Further evidence for bifurcation at St. Lawrence Island exists in transects B (Fig. 1.9) and D (Fig. 1.11), across Anadyr and Shpanberg Straits, and transect C (Fig. 1.10), located on the south side of the island (July 1985). AW was present in all transects (Figs. 1.9-1.11), as evidenced by the presence of >32.7 ppt salinity. During transit south of St. Lawrence Island, the maximum chlorophyll concentrations found in the transects remain constant but there is a dramatic decrease in the maximum nitrate concentrations. From Anadyr Strait to Shpanberg Strait, the maximum nitrate concentration was reduced by $16 \mu\text{g-at N} \cdot \text{L}^{-1}$ by both diffusive loss and biological fixation. Springer (1988) has reported carbon uptake rates of over $2 \text{ g C} \cdot \text{m}^{-2} \cdot \text{d}^{-1}$ at stations located in the western end of Shpanberg Strait. Because there is no evidence of chlorophyll accumulation during transit, plant production resulting from nitrate uptake must be grazed in the water column or lost to the benthos. Both loss terms are likely but the relative importance of each is unknown.

Transit Through Anadyr and Shpanberg Straits

Throughout the summer season, most plant material transported through Anadyr and Shpanberg Straits is found within the salinity envelope that defines Shelf water (31.5-32.7 ppt). The general summer distribution of bottom salinity provides a view of the path taken by Shelf water (Fig. 1.12). To trace the plant material that is produced south of St. Lawrence Island and transported into the area, chlorophyll *a* concentrations were integrated from below the approximate depth of the pycnocline (15 m) to the bottom, thus excluding plant material locally produced at the surface. It is clear that the chlorophyll *a* concentration (integrated from 15 m to the bottom) outlines the same path as the Shelf water salinity envelope (Fig. 1.13). Plant material within Shelf water is transported through the straits throughout the summer season (Fig. 1.14), decreasing in concentration by mid-October. It is likely that plant material transport begins in late May or early June, when shelf break production is initiated (Fig. 1.4).

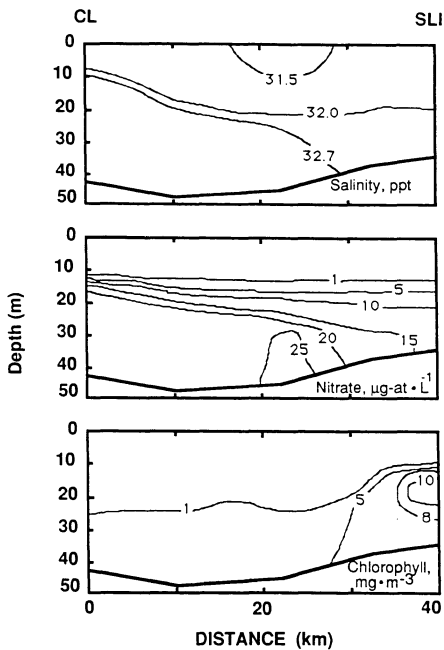


Figure 1.9 Vertical cross-sections from Transect B in July 1985. The transect originates at the U.S.-U.S.S.R. convention line (CL) and terminates at St. Lawrence Island (SLI).

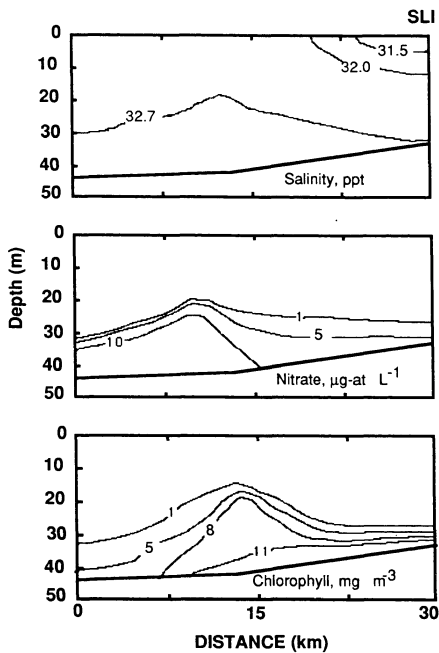


Figure 1.10 Vertical cross-sections from Transect C in July 1985. The transect originates at St. Lawrence Island (SLI) and terminates south of the island.

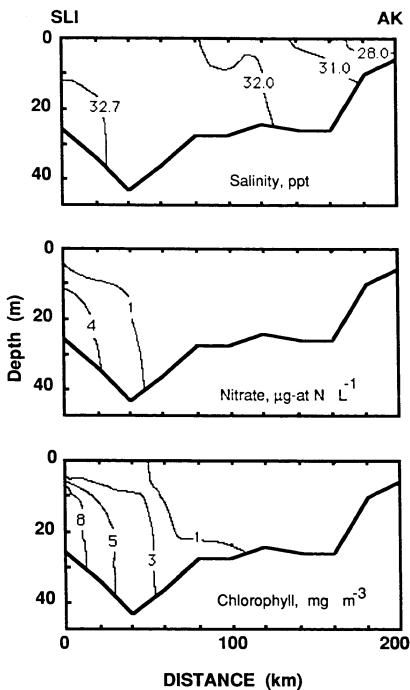


Figure 1.11 Vertical cross-sections from Transect D in July 1985. The transect originates at St. Lawrence Island (SLI) and terminates near the Alaskan coast (AK).

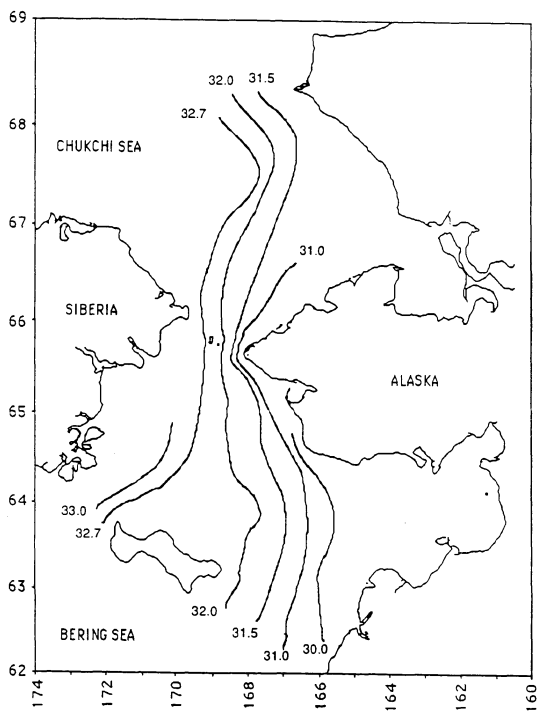


Figure 1.12 Distribution of bottom salinity (ppt) in July 1987.

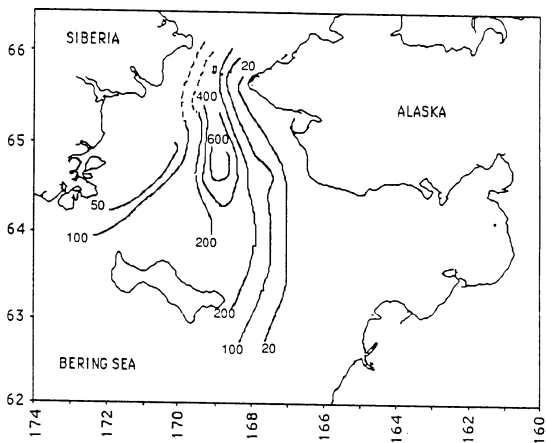


Figure 1.13 Distribution of chlorophyll ($\text{mg}\cdot\text{m}^{-2}$) integrated from 15 m to the bottom (July 1987).

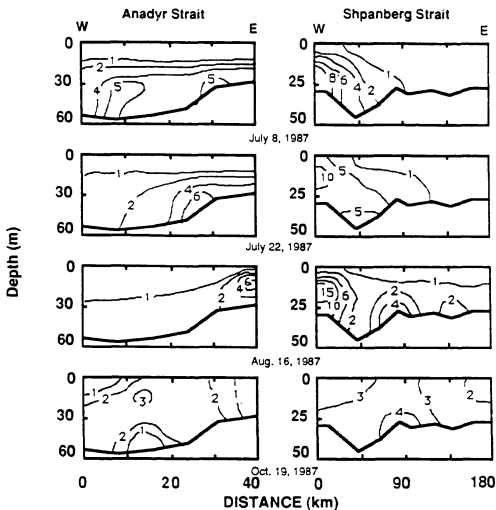


Figure 1.14 Vertical cross-sections of chlorophyll ($\text{mg}\cdot\text{m}^{-3}$) in Anadyr and Shpanberg Straits on four dates in summer 1987.

Deposition and Regeneration in the Northern Bering Sea

The Shelf water chlorophyll signal can be traced north across the Chirikov Basin and eventually through Bering Strait (Fig. 1.13). During its transit across the basin, large amounts of plant biomass must be deposited in the sediments as the source of carbon required by the rich amphipod beds found in the region. Grebmeier (1987) reports a benthic biomass of $20.2 \text{ g C} \cdot \text{m}^{-2}$ under Shelf water in the northern Bering Sea (10^{11} m^2), mostly dominated by detritus feeding amphipods, and estimates mean benthic organic carbon mineralization rates from July to September (1984 - 1986) to be $19.5 \text{ mmol C} \cdot \text{m}^{-2} \cdot \text{d}^{-1}$.

The estimate of the rate of carbon mineralization is equivalent to $38 \text{ mg N} \cdot \text{m}^{-2} \cdot \text{d}^{-1}$ of particulate nitrogen (PN), given an average C:N ratio (by weight) of 6.2 for the particulate fraction in Shelf water (Grebmeier, 1987). Assuming a 20% transfer efficiency in the benthos (Walsh, 1988), $47 \text{ mg N} \cdot \text{m}^{-2} \cdot \text{d}^{-1}$ are required to meet the measured mineralization rate. PN can be expressed as chlorophyll *a* concentration using a linear regression equation that describes the proportion of PN ($\mu\text{g-at N} \cdot \text{L}^{-1}$) to chlorophyll *a* ($\text{mg} \cdot \text{m}^{-3}$). For chlorophyll *a* below the pycnocline in Shelf water, $\text{PN} = 0.542 (\text{Chl}) + 1.338$ ($r^2 = 0.88$, $\text{df} = 173$). Approximately $3.1 \times 10^8 \text{ g chl } a \cdot \text{d}^{-1}$ must be available to meet the carbon demands of the benthos. Walsh *et al.* (in press) have estimated the mean Shelf water chlorophyll concentrations in 1987 to be $97 \text{ mg} \cdot \text{m}^{-2}$ and $80 \text{ mg} \cdot \text{m}^{-2}$ in Anadyr and Shpanberg Straits, respectively. Average summer transport was estimated to be 0.87 Sv and 0.31 Sv in the respective straits. The average depth of Shelf water in each strait is approximately 35 m , and Shelf water contributes approximately 30% of the total flow through each strait. From this, the mean flux of Shelf water chlorophyll through the straits is estimated at $0.8 \times 10^8 \text{ g chl } a \cdot \text{d}^{-1}$. Given the chlorophyll equivalent of benthic carbon consumption calculated above, the flux of biomass through Anadyr and Shpanberg Straits can meet approximately 26% of the daily carbon requirements of the Chirikov Basin benthos.

In July, 1987, maximum Shelf water chlorophyll concentrations were $<200 \text{ mg} \cdot \text{m}^{-2}$ when transiting Anadyr and Shpanberg Straits and increased to $>600 \text{ mg} \cdot \text{m}^{-2}$ over the Chirikov Basin (Fig. 1.13). The benthic amphipods are subsisting on the plant and detrital materials transported into the area with Shelf water and, in turn, are remobilizing nitrogen (ammonium and urea) from the particulate fraction (Lund and Blackburn, personal communication), thus stimulating new plant growth.

Production at the Shelf Break Front

Coachman and Walsh (1981) used a diffusion model to estimate the spring cross-shelf flux of nitrate and its rate of biological uptake in the southeastern Bering Sea during 1976 to 1979. Nitrate uptake rates of approximately $1.0 \mu\text{g-at NO}_3^- \cdot \text{L}^{-1} \cdot \text{d}^{-1}$ were calculated for the 1978 to 1979 spring euphotic zone of the outer shelf domain. Such a nitrate flux would be equivalent to $140 \text{ mg NO}_3^- \cdot \text{N} \cdot \text{m}^{-2} \cdot \text{d}^{-1}$ given a 10 m euphotic zone. At this time of year, zooplankton grazing stress results in ammonium fluxes that support 50% of the nitrogen demand of the phytoplankton (Hattori and Wada, 1974). Assuming that the ratio of C:N fluxes into the particulate fraction is 6:1, then $1.7 \text{ g C} \cdot \text{m}^{-2} \cdot \text{d}^{-1}$ would be fixed. During a 120 day growing season, this would result in a summer production of $204 \text{ g C} \cdot \text{m}^{-2}$ over the $1000 \text{ km} \times 50 \text{ km}$ shelf break. Goering and Iverson (1978) reported production rates of $2.3\text{-}5.2 \text{ g C} \cdot \text{m}^{-2} \cdot \text{d}^{-1}$ at four shelf break front stations in the southeast Bering Sea in May, 1978.

Surface Blooms in the ISHTAR Area

East Bloom - As would be expected, the Shelf water bottom chlorophyll mass is to some extent light limited. Though Shelf water is often capped by low salinity water (except in regions of very close proximity to St. Lawrence Island) as it enters the ISHTAR study area, it often can be found near the surface north of the island. Where Shelf water is near-surface ($<15 \text{ m}$ depth), significant accumulations of chlorophyll a may be found (Fig. 1.15, Station 42). This surface accumulation is here referred to as the east bloom. The east bloom is clearly a surface extension

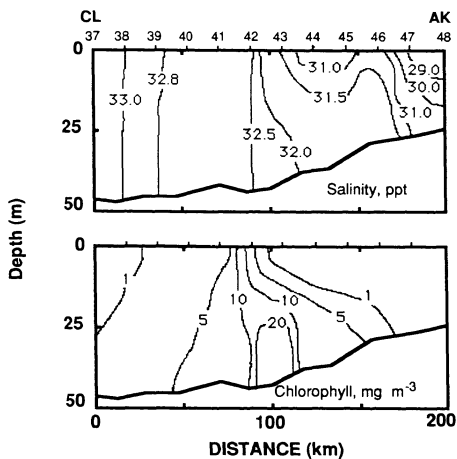


Figure 1.15 Vertical cross-sections from Transect E in July 1987. The transect originates at the U.S.-U.S.S.R. convention line (CL) and terminates near the Alaskan coast (AK).

of Shelf water (Fig. 1.15, Station 43) that has been transported through Anadyr and Shpanberg Straits.

The east bloom is relatively narrow (10 km), originating north of St. Lawrence Island, at the west end of Shpanberg Strait, and terminating (see below) in the Bering Strait, with a surface area of approximately 500-1000 km² (Fig. 1.16). Daily carbon production during August, 1987, ranged from 0.95 to 7.4 g C · m⁻² · d⁻¹, with a mean of 2.8 g C · m⁻² · d⁻¹ (Springer, personal communication).

West Bloom - As discussed above, Anadyr water is continuously upwelled into the ISHTAR study area through Anadyr Strait. It is cold, high salinity water (>32.7 ppt) characterized by high nitrate concentrations (>25 µg-at N · L⁻¹). Immediately north of Anadyr Strait, Anadyr water often can be found well mixed from surface to bottom. Further north of the strait, Anadyr water typically is overlain by Shelf water or Siberian Coastal water.

Where Anadyr water remains well mixed to the surface, no surface bloom has been found to develop (Fig. 1.15, Stations 37-39). This is because the plant cells, though well supplied with nutrients, are mixed out of the euphotic zone at a frequency preventing net production (Sverdrup, 1953). Near-surface Anadyr water is eventually capped by low salinity water (<32.0 ppt), thus providing the requisite stability for bloom production (Fig. 1.17, Station 56). Because of the high concentration of nitrate in Anadyr water, a strong nitrate gradient exists (23 µg-at N L⁻¹) between Anadyr water and the overlying low nutrient, low salinity water. This gradient supports diffusive export of Anadyr water nitrate into the surface lens. Hence, at the pycnocline, enhanced plant production can be found (McRoy *et al.*, 1987). Where capping of Anadyr water was followed by bloom development, the greatest rate of plant production and the greatest surface (0-15 m) concentrations of plant biomass (here referred to as the west bloom) were measured in 1987 (Fig. 1.16).

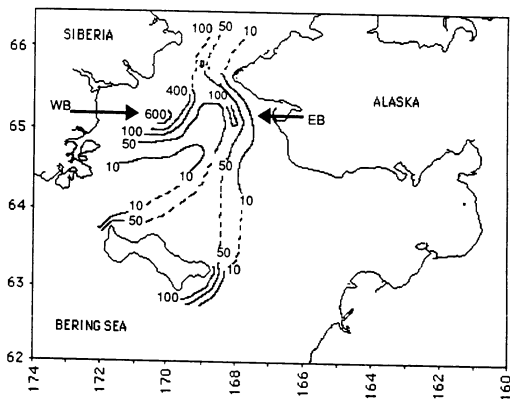


Figure 1.16 Distribution of chlorophyll ($\text{mg} \cdot \text{m}^{-2}$) integrated from the surface to 15 m. The east (EB) and west (WB) blooms are indicated.

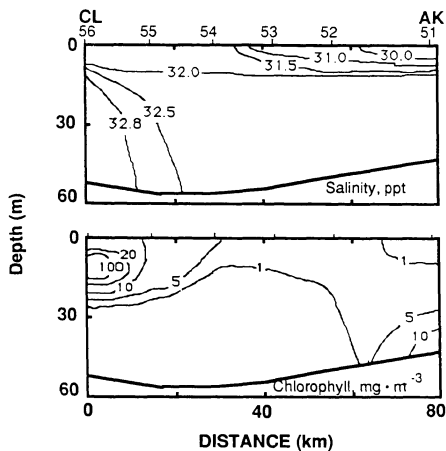


Figure 1.17 Vertical cross-sections from Transect G in August 1987. The transect originates at the U.S.:U.S.S.R. convention line (CL) and terminates near the Alaskan coast (AK).

Chlorophyll distribution and primary production in the west bloom has been described for years 1985-1987 (Springer, 1988). Carbon uptake rates measured within the west bloom ranged between 1 and $16 \text{ g C} \cdot \text{m}^{-2} \cdot \text{d}^{-1}$, while outside the west bloom rates were usually less than $1 \text{ g C} \cdot \text{m}^{-2} \cdot \text{d}^{-1}$. The area south of Bering Strait that was defined as the west bloom averaged $0.87 \times 10^{10} \text{ m}^2$. The average daily production for the west bloom was estimated to range from 1.5 - $5.4 \text{ g C} \cdot \text{m}^{-2} \cdot \text{d}^{-1}$, with a mean of $2.7 \text{ g C} \cdot \text{m}^{-2} \cdot \text{d}^{-1}$. This is equivalent to mean production in the east bloom; however, the west bloom is estimated to be approximately 9-18 fold greater in surface area than the east bloom.

Still higher production would be anticipated following transit of the west bloom through Bering Strait into the southern Chukchi, where surface chlorophyll concentrations (0 - 15 m) of $> 800 \text{ mg} \cdot \text{m}^{-2}$ can be found, and carbon production as high as $16 \text{ g C} \cdot \text{m}^{-2} \cdot \text{d}^{-1}$ has been reported (Springer, 1988). Unfortunately, the west bloom is often not available for direct observation during passage through Bering Strait due to the limitations set by the US-USSR 1867 Convention Line. The east bloom, too, flows northwest across the convention line into Soviet territory at Bering Strait and becomes unavailable for direct observation. Where the west bloom reenters American territory north of Bering Strait, the east bloom is no longer in evidence, suggesting that the two blooms have merged (Fig. 1.16). The distribution of east and west bloom chlorophyll is readily visible in a Coastal Zone Color Scanner image available in Walsh *et al.* (in press, their Fig. 19). The merged bloom, along with the Shelf water bottom chlorophyll that has transited Bering Strait, must be the primary source of carbon for the rich benthic populations found in the southern Chukchi Sea (Stoker, 1981; Grebmeier, 1987).

SUMMARY

General Model for Summer Production and Consumption on the Northern Bering Sea Shelf

A diagrammatic model of summer phytoplankton production and consumption on the northern Bering Sea shelf is presented in Fig. 1.18. The system of primary productivity found in the ISHTAR study area is the downstream continuation of the system of productivity located at the shelf break of the Bering Sea. Summer production in the northeastern Bering Sea is wholly dependent on the flux of nutrients from water comprising the Bering Slope/ Anadyr Currents into outer domain/ modified Bering shelf water. Production at the shelf break front is initiated in May, when water column stability maintains a light regime favorable for plant growth, and continues into the fall, when frequent wind mixing and cooling of the surface water column reduces net plant production.

Production associated with the shelf break front is estimated at approximately $204 \text{ g C} \cdot \text{m}^{-2}$ over the 120-day growing period. Near-bottom chlorophyll concentrations are $<1 \text{ mg} \cdot \text{m}^{-3}$ (Fig. 1.6) and sinking rates of phytoplankton are estimated to be $1 \text{ m} \cdot \text{day}^{-1}$ at the shelf break front (Iverson *et al.*, 1979b). Consequently, shelf break production is diverted directly to the pelagic food web of the outer shelf domain throughout the summer.

The Bering Slope Current bifurcates at Cape Navarin and, now referred to as the Anadyr Current, crosses the Gulf of Anadyr, passing north through Anadyr and Bering Straits. A portion of the biomass accumulated above the shelf break front is diverted to the north with the Anadyr Current and, as part of the Shelf water mass, bifurcates at St. Lawrence Island. The biomass transported around St. Lawrence Island supplies 26% of the daily carbon demand of the rich amphipod beds located in the Chirikov Basin, south of Bering Strait. During shoaling of Shelf water from the shelf break (200 m) to Chirikov Basin ($<50 \text{ m}$), a transition is made from a predominantly pelagic food web to one that is directly tied to the benthos.

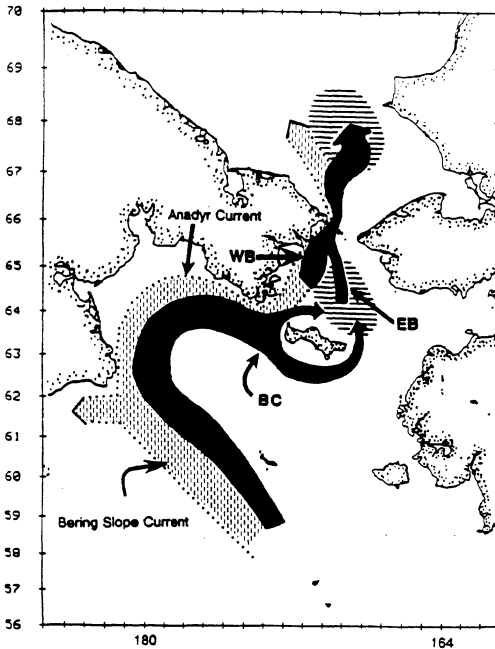


Figure 1.18 Generalized model for the production and transport of plant biomass associated with the Bering Slope and Anadyr Currents. Black zones represent the regions of plant biomass production and transport. Horizontal lines represent regions of deposition and vertical lines represent the Bering Slope and Anadyr Currents. The west and east blooms are labeled WB and EB, respectively. Plant biomass transported within the modified Bering Shelf water mass is labeled BC.

The Anadyr Current shoals at the shallow Anadyr Strait and an intense surface bloom (west bloom) develops north of the strait as a result of the sudden influx of nitrate to the euphotic zone. The west bloom is strongly advected to the north through Bering Strait, where it is joined by the east bloom, to be deposited in the benthos of the southern Chukchi Sea. Fig. 1.19 depicts diagrammatically the relative positions of the Anadyr, Shelf, Siberian Coastal, and Alaskan Coastal water masses in a latitudinal cross-section north of St. Lawrence Island and the associated accumulations of phytodetritus (west bloom, east bloom, and deep chlorophyll layer).

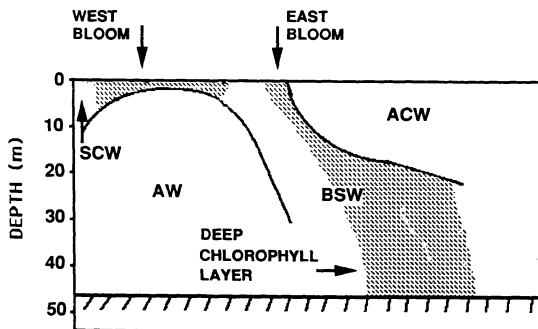


Figure 1.19 Diagrammatic latitudinal cross-section, situated north of St. Lawrence Island and south of Bering Strait, depicting relative positions of the water masses. Siberian Coastal water (SCW), Anadyr water (AW), modified Bering Shelf water (BSW), and Alaskan Coastal water (ACW) are indicated. Hatched areas represent regions of plant biomass accumulation.

CHAPTER 2: PELAGIC NITROGEN FLUX IN THE NORTHERN BERING SEA

INTRODUCTION

In the past, extensive studies of the nitrogen cycle in the waters overlying the Bering Sea continental shelf have been limited to springtime events in the southeastern Bering Sea such as the spring bloom (Sambrotto *et al.*, 1986) and the ice-edge bloom (Muller-Karger and Alexander, 1987). Nitrogen productivity data, in particular, is limited for the northern Bering Sea (McRoy *et al.*, 1972; Sambrotto *et al.*, 1984). However, estimates (Sambrotto *et al.*, 1984; Springer, 1988) of the annual rate of carbon production ($324 \text{ g C} \cdot \text{m}^{-2}$) suggest that portions of the northern Bering Sea have greater annual primary production than other shelf regions with western boundary currents (the Anadyr Current) and the estimated production is several-fold greater than other shelves located in high latitudes (Walsh, 1988).

In this chapter, nitrogen productivity rates measured as part of the Inner Shelf Transfer and Recycling (ISHTAR) program in the northern Bering and southern Chukchi Seas are discussed in the context of the water masses (Siberian Coastal, Anadyr, modified Bering Shelf and Alaskan Coastal) and regions of plant biomass accumulation (west and east blooms and the deep chlorophyll layer) characteristic of the region (see Chapter 1). I examine the importance of new (nitrate) versus regenerated (urea and ammonium) nitrogen productivity in each of the water masses. Finally, a simple nitrogen budget demonstrates that a significant portion of nitrogen productivity in the northern Bering Sea is exported into the Chukchi Sea via Bering Strait.

METHODS

The field work was carried out aboard the R/V *T. G. Thompson* from July 20 to September 31, 1987 (consecutive cruises TT213 and TT214). Sampling was restricted

to the east (American) side of the United States-Soviet Union convention line that divides the Bering Sea in the ISHTAR study area.

At all stations (hydrographic stations), water column conductivity and temperature were profiled with a Neil Brown CTD (i.e., an instrument equipped with conductivity, temperature, and pressure sensors). Water samples were collected in 5-L Niskin bottles at 5 m intervals to the bottom of the water column. Subsamples from each depth were analyzed for chlorophyll *a* and dissolved nutrients. Chlorophyll *a* content was determined on a Turner-Designs fluorometer by measuring the fluorescence of acetone extracts of particulate matter (Parsons *et al.*, 1984). Nutrient samples were collected for the determination of nitrate, ammonium and urea concentrations (diacetyl monoxime method) according to the methods of Whittledge *et al.* (1981). Samples were analyzed within 1 h of collection using automated techniques. Hydrographic, nutrient, and chlorophyll data were taken from ISHTAR Data Reports No. 1 (1985) and 9 (1987).

At selected stations (productivity stations), nitrogen productivity measurements were performed using ^{15}N -labelled nitrate, ammonium, and urea according to the method of Dugdale and Goering (1967). Uptake rates were calculated using Equation 3.1 (sample calculations can be found in Table 3.1). Samples were collected in a 30-L Niskin bottle from euphotic zone depths corresponding to 100, 50, 30, 15, 3, 1, and 0.1% of surface incident photosynthetically active radiation (PAR) as determined with a Licor LI-185 deck unit and a LI-192S underwater sensor. The water from each depth was prefiltered through a 333- μm Nitex® screen into three 2.27-L polycarbonate bottles screened with a neutral density filter (Perforated Products, Inc., nickel screens) to simulate the *in situ* light intensity. Three bottles were filled from each depth. With each ^{15}N -labelled nutrient (99 atom % ^{15}N -urea, 98 atom % ^{15}N -potassium nitrate, 99 atom % ^{15}N -ammonium chloride; Icon Services, Inc.), a bottle

was spiked to a final ^{15}N -atom % enrichment of <20%. Nutrient additions were made prior to completion of nutrient analysis to minimize the time between sample collection and the start of incubations.

Samples were incubated for 4-6 h on deck in Plexiglas® incubators purged with surface seawater and then filtered onto a precombusted (450°C) 0.6- μm quartz filter and rinsed with filtered seawater. The filters were dried at 50°C for 24 h and transported in a desiccator to the laboratory where they were combusted at 800°C for 4 h with approximately 1 g of Cuprox® in evacuated and sealed quartz tubes. Particulate nitrogen (PN) was determined from the pressure of N_2 measured with an MKS Type 122A Absolute Pressure Transducer after breaking the sealed quartz tubes in a high-vacuum manifold connected to an AEI MS20 dual collector mass spectrometer, on which isotope ratio analyses were performed. The coefficient of variation for the ratio of N_2 mass to transducer voltage (determination of PN) and the standard deviation for isotope ratio analyses (natural abundance samples) were typically <0.5% and 0.001 atom %, respectively. Corrections were not made for the effect of isotope dilution on the measurement of uptake rates of ammonium (Glibert *et al.*, 1982) or urea (Chapter 3). This causes an overestimate of the percent new production, and an underestimate of the uptake rates of urea and ammonium.

RESULTS AND DISCUSSION

Stations occupied during cruises TT213 and TT214 were located to enable study of the most hydrographically and biologically interesting features that existed during each cruise (Fig. 2.1). Cruise TT213 stations were located to cover the distributions of the water masses, the deep chlorophyll layer in the Bering Sea, and of both surface and deep distributions of chlorophyll in the Chukchi Sea. The west bloom was not in

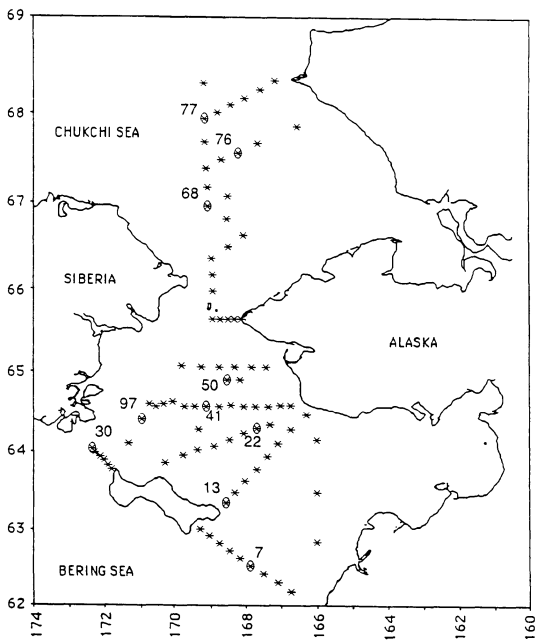


Figure 2.1a Locations of stations occupied in 1987 during TT 213. Productivity stations are numbered.

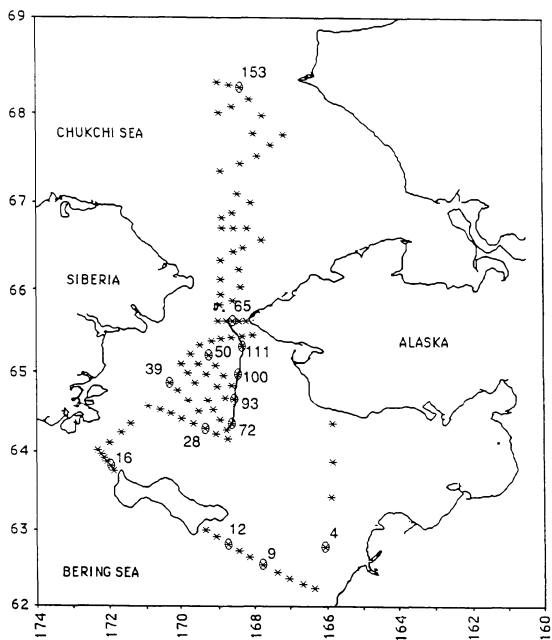


Figure 2.1b Locations of stations occupied in 1987 during TT 214. Productivity stations are numbered. The solid line represents a drogue track.

American waters during TT213. However, the east bloom and a portion of the west bloom were available for study during TT214.

Anadyr Water and the West Bloom

The distribution of bottom salinity during TT213 is presented in Fig. 1.12. Anadyr water (>32.7 ppt) was located to the west in Anadyr Strait and could be traced through Bering Strait into the southern Chukchi Sea. During TT213, integrated nitrate concentrations in Anadyr water south of Bering Strait ranged from 500 to >1000 mg-at $\text{NO}_3^- \cdot \text{N} \cdot \text{m}^{-2}$ (Fig. 2.2), while in the Chukchi Sea maximum integrated concentrations in Anadyr water were depleted to <500 mg-at $\text{NO}_3^- \cdot \text{N} \cdot \text{m}^{-2}$. Near-surface (10 m depth) concentrations of >15 $\mu\text{g-at } \text{NO}_3^- \cdot \text{N} \cdot \text{L}^{-1}$ were present during both cruises in the Bering Sea with up to 25 $\mu\text{g-at } \text{NO}_3^- \cdot \text{N} \cdot \text{L}^{-1}$ present during TT 214.

In July-August (TT 213), the west bloom was discernable only in the southern Chukchi Sea (Fig. 2.3) where integrated chlorophyll *a* values were over 1500 mg chl *a* $\cdot \text{m}^{-2}$. South of Bering Strait, the distribution of chlorophyll (Fig. 2.3) was most strongly influenced by the distribution of the deep chlorophyll layer (Fig. 1.13) since the west bloom was not in American waters. However, in September (TT 214) the distribution of chlorophyll near the surface (integrated 0-15 m) did highlight features common to Anadyr water. For instance, low chlorophyll concentrations (<10 mg $\cdot \text{m}^{-2}$) were present within and north of Anadyr Strait where Anadyr water was well-mixed to near-surface (Fig. 1.16). High surface chlorophyll concentrations (>600 mg $\cdot \text{m}^{-2}$), comprising the west bloom, were found immediately downstream of the low chlorophyll area in a region of increased surface buoyancy. Further downstream, in the Chukchi Sea, surface concentrations (integrated 0-15 m) rose to >800 mg $\cdot \text{m}^{-2}$ during TT 214. This condition is analogous to the prebloom and bloom stages of phytoplankton development described by Sambrotto *et al.* (1986) for the spring bloom in the middle

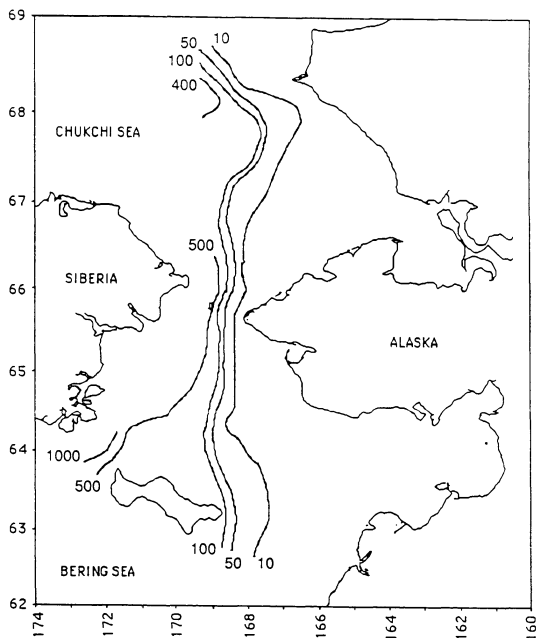


Figure 2.2 Distribution of integrated nitrate ($\text{mg-at N}\cdot\text{m}^{-2}$; redrawn from Springer, 1988) during TT 213.

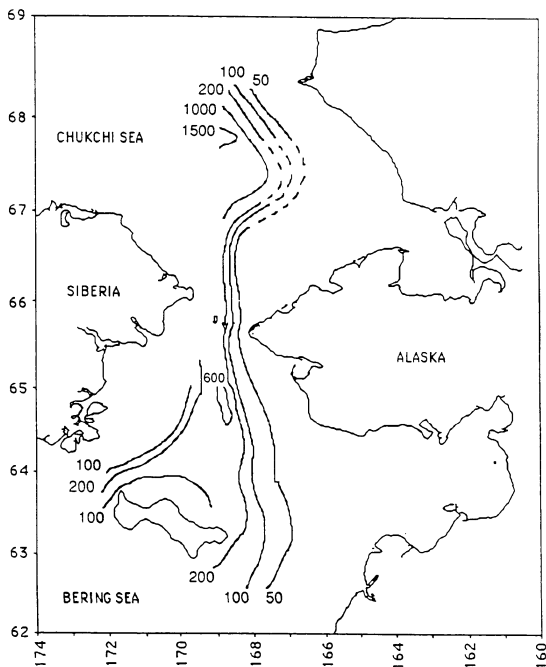


Figure 2.3 Distribution of integrated chlorophyll ($\text{mg chl } a \cdot \text{m}^{-2}$; redrawn from Springer, 1988) during TT 213.

shelf of the southeastern Bering Sea. In that region, the shallowing of the mixed layer was important to initiation of bloom conditions and it is likely that similar buoyancy requirements must be met in the northern Bering Sea. However, in the strongly advective ISHTAR study area, there is a spatial separation of the developmental stages in a phytoplankton bloom. Because of the spatial separation, there can exist throughout the summer season a continuous prebloom condition in the region of Anadyr Strait, followed by a continuous bloom condition further downstream.

Where Anadyr water was well-mixed to near-surface, and no surface accumulation of chlorophyll was evident (prebloom Anadyr water), total nitrogen (nitrate, ammonium, and urea combined) productivity rates were $<1.4 \text{ mg-at N} \cdot \text{m}^{-2} \cdot \text{h}^{-1}$ (Table 2.1). Nitrate-based productivity represented $> 60\%$ of the total on average and, at one station, was 80%. Cochlan (1986) reported a 67% contribution by nitrate to total nitrogen uptake during winter on the Scotian Shelf, while during spring and summer, the importance of nitrate decreased to 27% and 30%, respectively.

In the west bloom, nitrogen productivity was, on average, 3.18 and 6.11 $\text{mg-at N} \cdot \text{m}^{-2} \cdot \text{h}^{-1}$ (47.7 and 91.6 $\text{mg-at N} \cdot \text{m}^{-2} \cdot \text{d}^{-1}$ assuming a 15 h day) south and north of Bering Strait, respectively. Nitrate-based production averaged $<50\%$ of the total in the west bloom. Previous measurements of nitrate uptake in the area of the west bloom indicated rates ranging from $>5 \text{ mg-at NO}_3\text{-N} \cdot \text{m}^{-2} \cdot \text{d}^{-1}$ (McRoy, 1983) to more than 20 $\text{mg-at NO}_3\text{-N} \cdot \text{m}^{-2} \cdot \text{d}^{-1}$ (McRoy *et al.*, 1972) in western Bering Strait where percent nitrate uptake ranged from 77 to 89% of total nitrogen productivity above the 10% light depth. However, urea uptake was not considered in that work.

Station 97 (TT213), located in recently upwelled Anadyr water, provides an example of high salinity deep water, capped by Siberian Coastal water, exhibiting low

Table 2.1. The range and mean of total nitrogen productivity (nitrate, ammonium, and urea uptake combined) and the contribution of nitrate, ammonium, and urea to productivity within biological regimes characteristic of the water masses located in the 1987 ISHTAR study area. Standard deviations are in parentheses. N is the number of stations.

Water Mass	Nitrogen Productivity (mg-at N m ⁻² h ⁻¹)					
	Range	Mean	N	NO ₃ ⁻ (%)	NH ₄ ⁺ (%)	Urea (%)
Anadyr						
prebloom	0.76 - 1.40	1.01 (0.25)	5	63.8	20.9	15.3
West Bloom						
-south of Bering Strait	2.52 - 3.89	3.18 (0.66)	4	38.1	20.2	41.7
-north of Bering Strait	6.02 - 6.20	6.11 (0.13)	2	49.7	34.6	15.7
Modified Bering Shelf						
East Bloom	1.20 - 2.52	1.81 (0.54)	5	35.0	34.9	30.1
non-bloom	0.74 - 3.00	1.80 (0.75)	10	27.0	47.7	25.3
Alaskan Coastal	0.65 - 1.48	1.03 (0.42)	3	14.9	47.7	37.4

PN concentrations (Fig. 2.4). The water column was rich in nutrients ($> 17.0 \mu\text{g-at NO}_3^- \cdot \text{N} \cdot \text{L}^{-1}$ at the surface), yet PN concentrations at all depths were $< 1.5 \mu\text{g-at N} \cdot \text{L}^{-1}$. The total nitrogen specific uptake rates were greatest near the surface (0.021 h^{-1}) and decreased by only 28% at the 0.1% light depth. The integrated productivity rate for total nitrogen at this station was $0.84 \text{ mg-at N} \cdot \text{L}^{-1} \cdot \text{h}^{-1}$.

Station 39 (TT214) was characteristic of stations located in the west bloom (Fig. 2.5). A shallow surface lens (0-5 m) contained high PN concentrations ($6.6\text{--}11.3 \mu\text{g-at N} \cdot \text{L}^{-1}$) while below the halocline low PN values ($< 2.0 \mu\text{g-at N} \cdot \text{L}^{-1}$) were present in very high salinity water. The nitrate concentration was $> 13 \mu\text{g-at N} \cdot \text{L}^{-1}$ at the surface and increased to $24 \mu\text{g-at N} \cdot \text{L}^{-1}$ at depth. The integrated uptake rate of total nitrogen at this station ($3.89 \text{ mg-at N} \cdot \text{L}^{-1} \cdot \text{h}^{-1}$) was 460% greater than the rate measured at Station 97, located in prebloom Anadyr water.

Modified Bering Shelf Water, Deep Chlorophyll, and the East Bloom

The salinity range for Shelf water during 1987 was approximately 31.5 - 32.7 ppt. Its path could be traced from east and west of St. Lawrence Island, north through Bering Strait, and into the Chukchi Sea (Fig. 1.12). Integrated nitrate concentrations ranged from approximately 100 to $500 \text{ mg-at NO}_3^- \cdot \text{N} \cdot \text{m}^{-2}$ (Fig. 2.2) with near-surface concentrations reduced from $< 5 \mu\text{g-at NO}_3^- \cdot \text{N} \cdot \text{L}^{-1}$ in the Bering Sea to $< 1 \mu\text{g-at NO}_3^- \cdot \text{N} \cdot \text{L}^{-1}$ in the Chukchi Sea.

A distinctive accumulation of surface chlorophyll in Shelf water, located to the east of the west bloom, is referred to as the east bloom (Chapter 1). Surface chlorophyll concentrations (integrated 0-15 m) in the east bloom ranged from 50 to $> 100 \text{ mg} \cdot \text{m}^{-2}$ (Fig. 1.16). In the deep chlorophyll layer (TT 213), concentrations of chlorophyll (integrated 15 m to bottom) were $> 100 \text{ mg} \cdot \text{m}^{-2}$ in Anadyr and Shpanberg

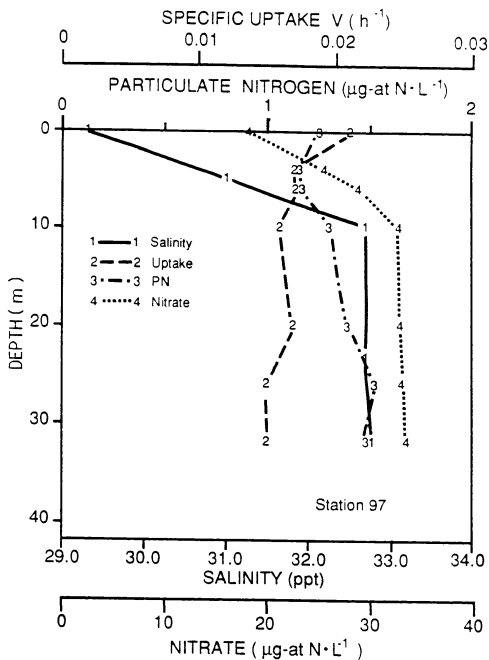


Figure 2.4 Depth distribution of salinity (ppt), total nitrogen (nitrate, ammonium, and urea combined), specific uptake rates (h^{-1}), particulate nitrogen and nitrate ($\mu\text{g-at N} \cdot \text{L}^{-1}$) for productivity Station 97.

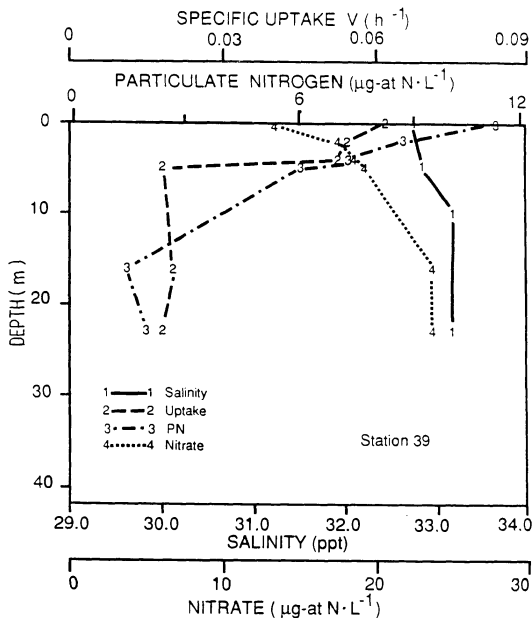


Figure 2.5 Depth distributions of salinity (ppt), total nitrogen (nitrate, ammonium, and urea combined) specific uptake rates (h^{-1}), particulate nitrogen and nitrate ($\mu g-at N \cdot L^{-1}$) for productivity Station 39.

Straits and reached values of >600 (Fig. 1.13) and $>1400 \text{ mg} \cdot \text{m}^{-2}$ in the Bering and Chukchi Seas, respectively.

Total nitrogen productivity rates in Shelf water were approximately 70% greater than those measured in prebloom Anadyr water (Table 2.1), reflecting both higher specific uptake rates and greater PN concentrations. However, the contribution of nitrate to the total nitrogen consumed was halved from 64% in Anadyr water to 26.8%. East bloom total nitrogen productivity rates ($1.81 \text{ mg-at N} \cdot \text{m}^{-2} \cdot \text{h}^{-1}$) were of the same magnitude as other Shelf water regions.

Station 13 (TT214), located near St. Lawrence Island in the region of Shpanberg Strait (Fig. 2.1), exhibited a PN depth profile that was consistent with the characteristics described for the deep chlorophyll layer. PN increased to $>6.0 \text{ } \mu\text{g-at N} \cdot \text{L}^{-1}$ at the depth of the halocline and remained relatively constant to the bottom (Fig. 2.6). The surface water, the salinity of which was characteristic of Alaskan Coastal water (<31.5 ppt), was depleted of nitrate ($<0.1 \text{ } \mu\text{g-at N} \cdot \text{L}^{-1}$) and had PN concentrations of approximately $2 \text{ } \mu\text{g-at N} \cdot \text{L}^{-1}$. The specific uptake rate of total nitrogen was greatest near the surface ($0.030 \text{ } \mu\text{g-at N} \cdot \text{L}^{-1} \cdot \text{h}^{-1}$) and decreased to a relatively constant value ($0.011 \text{ } \mu\text{g-at N} \cdot \text{L}^{-1} \cdot \text{h}^{-1}$) with depth. The absolute uptake rate of total nitrogen was maximal near the halocline and the integrated nitrogen productivity rate was $2.51 \text{ mg-at N} \cdot \text{L}^{-1} \cdot \text{h}^{-1}$.

In Chapter 1 I argued that the deep chlorophyll layer is the downstream continuation of the system that produced phytodetritus at the shelf break front in the Bering Sea. Goering and Iverson (1978) reported production rates of $2.3\text{-}5.2 \text{ g C} \cdot \text{m}^{-2} \cdot \text{d}^{-1}$ at four shelf break stations in May 1978. Assuming a 15 h day and a C:N uptake ratio of 6, the reported rates are equivalent to $2.1\text{-}4.8 \text{ mg-at N} \cdot \text{m}^{-2} \cdot \text{h}^{-1}$, a range which overlaps our measured values (Table 2.1).

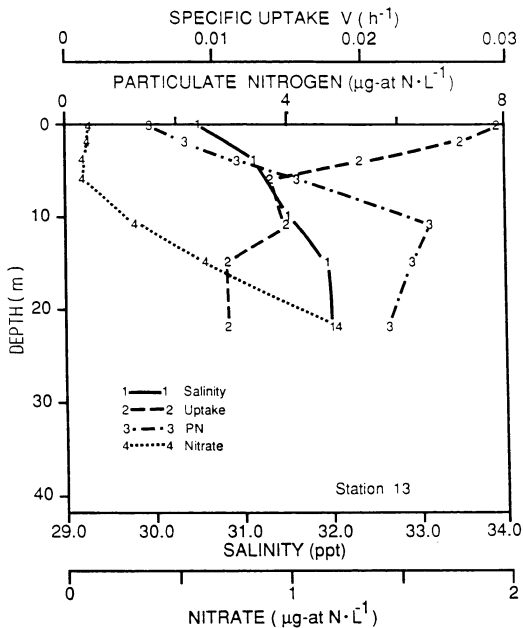


Figure 2.6 Depth distribution of salinity (ppt), total nitrogen (nitrate, ammonium, and urea combined), specific uptake rates (h^{-1}), particulate nitrogen and nitrate ($\mu\text{g-at N} \cdot \text{L}^{-1}$) at productivity Station 13.

Typical depth profiles of PN and nitrogen uptake for a station located in the east bloom (Station 111, TT214) are presented in Fig. 2.7. Particulate nitrogen concentrations were $>6.0 \mu\text{g-at N} \cdot \text{L}^{-1}$ in the surface 8 m and decreased to $<3.0 \mu\text{g-at N} \cdot \text{L}^{-1}$ near the bottom of the euphotic zone. The specific uptake rate was nearly constant with depth, resulting in an integrated nitrogen productivity rate of $1.81 \text{ mg-at N} \cdot \text{L}^{-1} \cdot \text{h}^{-1}$. The nitrate concentration was low, ranging from approximately $1.5 \mu\text{g-at N} \cdot \text{L}^{-1}$ at the surface to $<3.0 \mu\text{g-at N} \cdot \text{L}^{-1}$ at depth.

Alaskan Coastal Water

Alaskan Coastal water salinity was generally <31.5 ppt in 1987. It followed the contour of the Alaskan coast through Bering Strait into the southern Chukchi Sea (Fig. 1.12). During TT213, integrated nitrate concentrations were $<10 \text{ mg-at NO}_3^- \cdot \text{N} \cdot \text{m}^{-2}$ and integrated chlorophyll concentrations were $<30 \text{ mg} \cdot \text{m}^{-2}$ (Fig. 2.2). Combined nitrogen productivity rates were approximately $1.0 \text{ mg-at N} \cdot \text{m}^{-2} \cdot \text{h}^{-1}$ on average and nitrate contributed only 15% to the total uptake (Table 2.1). Previous nitrate uptake measurements performed in Alaskan Coastal water resulted in rates of less than $1 \text{ mg-at NO}_3^- \cdot \text{m}^{-2} \cdot \text{d}^{-1}$ (McRoy, 1983).

Contribution of Regenerated Nutrients

The relative contributions of ammonium and urea to total nitrogen productivity in the ISHTAR area varied with the magnitude of productivity (Table 2.1). Urea uptake was approximately equivalent to that of ammonium where productivity was lowest. For instance, in both prebloom Anadyr water and Alaskan Coastal water the contributions of urea and ammonium were within 5 and 10% of each other, respectively. However, the contribution of regenerated nitrogen to total production was far less in Anadyr water where nitrate concentrations were high ($> 15 \mu\text{g-at N} \cdot \text{L}^{-1}$), than in coastal water where the concentration of nitrate was low ($< 0.5 \mu\text{g-at N} \cdot \text{L}^{-1}$).

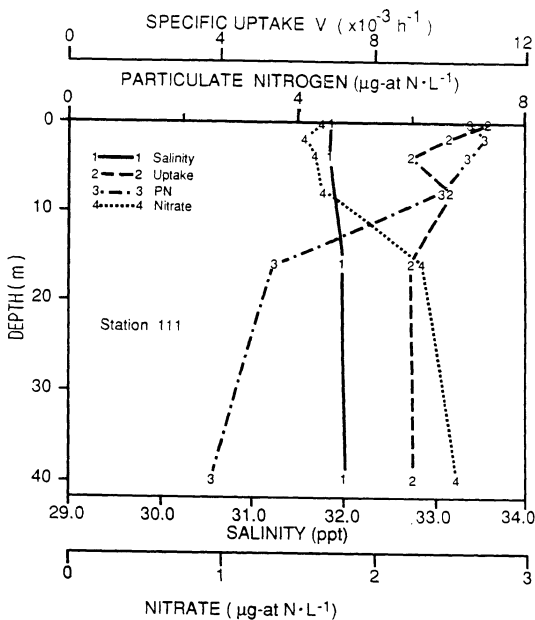


Figure 2.7 Depth distributions of salinity (ppt), total nitrogen (nitrate, ammonium, and urea combined) specific uptake (h^{-1}), particulate nitrogen and nitrate ($\mu\text{g-at N} \cdot \text{L}^{-1}$) at productivity Station 111.

In the highly productive waters of the west bloom, the contribution of regenerated nutrients was 50-60% of total production but the individual contributions of ammonium and urea were not equivalent. South of Bering Strait, urea was most important in meeting the nitrogen demands of the phytoplankton, while north of the strait ammonium was more important. This observation is based on a very limited number of stations (only two north of the strait) so conclusions must be developed with caution.

Price *et al.* (1985) evaluated the uptake of nitrate, ammonium, and urea in frontal and stratified waters in the Strait of Georgia (British Columbia), which may be comparable to the conditions in the ISHTAR area. As with our results, in frontal systems rich with nitrate (our prebloom area), the specific uptake rates of nitrate were greater than the uptake rate of the regenerated nutrients. The converse was true for stratified waters. Alaskan Coastal and Shelf waters, being depleted of nitrate, were similar to the stratified waters studied by Price *et al.* (1985). In these water masses, regenerated nutrients played the most significant role in supplying nitrogen to the phytoplankton community.

Estimation of Nitrogen Productivity in Shelf Water

To estimate nitrogen productivity at all stations located in Shelf water during TT213, we first identified stations exhibiting our criterion for Shelf water (salinity >31.5 ppt and <32.7 ppt) in some portion of the water column. Using data from TT213 and TT214 productivity stations located in Shelf water (N=7), the mean total nitrogen specific uptake rate from each %PAR depth (e.g., 50% PAR) was plotted against the mean depth (e.g., 2.1 m) from which the corresponding rate was determined (Fig. 2.8). From this depth curve, we estimated the mean specific uptake rate at depth increments of 5 m by linear interpolation between the data points. Nitrogen specific uptake rates

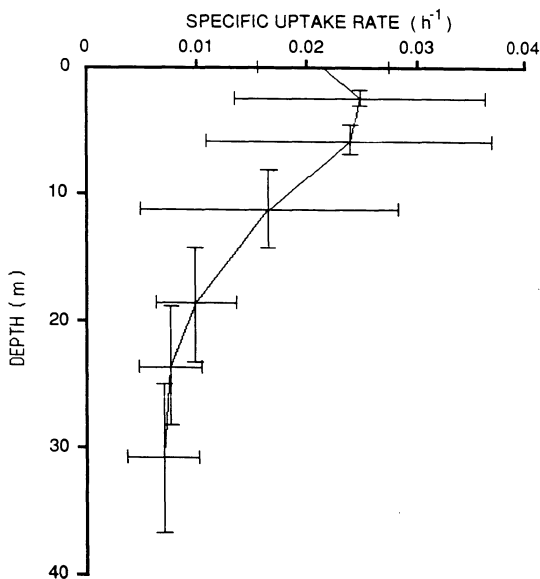


Figure 2.8 Mean depth (m) and mean total nitrogen (nitrate, ammonium, and urea combined) specific uptake rates (h^{-1}) for seven photosynthetically active radiation depths (100, 50, 30, 15, 3, 1.0, 0.1%) from seven productivity stations located in modified Bering Shelf water. Bars represent \pm one standard deviation.

estimated from the depth curve of mean specific uptake rates ranged from 0.0242 h^{-1} near the surface to a fairly constant 0.0070 h^{-1} with depth.

An estimate of PN at the same %PAR depths allows estimates of the absolute uptake rates of nitrogen. A linear regression equation was established in Chapter 1 describing the proportion of chlorophyll *a* ($\text{mg} \cdot \text{m}^{-3}$) to PN ($\mu\text{g-at N} \cdot \text{L}^{-1}$) in 1987 Shelf water, thereby permitting an estimation of PN at all Shelf water hydrographic stations. For Shelf water chlorophyll *a*, $\text{PN} = 0.542 (\text{chl } a) + 1.338$ ($r^2 = 0.88$, $\text{df} = 173$). At each hydrographic station, the PN estimated at 5-m depth intervals was multiplied by the nitrogen specific uptake rate estimated for that depth and the results were integrated over that portion of the water column defined as Shelf water. From the areal distribution of estimated nitrogen uptake rates, I determined the surface area between nitrogen productivity isopleths (0.25 - 1.0 , 1.0 - 1.5 , 1.5 - 2.0 , 2.0 - 3.0 , 3.0 - $3.25 \text{ mg-at N} \cdot \text{m}^{-2} \cdot \text{h}^{-1}$) for Shelf water south of Bering Strait and north of Shpanberg and Anadyr Straits. The median value within each isopleth pair was multiplied by the surface area of that pair. The resultant values were summed and then normalized to the total surface area of Shelf water (10^{11} m^2). This approach provides a mean uptake value that is weighted for the areal contribution to total production.

The mean nitrogen productivity rate over the region covered by Shelf water during TT213 is estimated to be $1.34 \text{ mg-at N} \cdot \text{m}^{-2} \cdot \text{h}^{-1}$. This value is 25% less than the mean for measured rates (Table 2.1). Based on a molar uptake ratio of 6, the mean carbon uptake rate was $0.096 \text{ g C} \cdot \text{m}^{-2} \cdot \text{h}^{-1}$. Assuming a 15 h day, the daily C fixation rate should be near $1.4 \text{ g C} \cdot \text{m}^{-2}$. Springer (1988) has estimated C uptake in all regions outside of the west bloom to be $<1 \text{ g C} \cdot \text{m}^{-2} \cdot \text{d}^{-1}$. Differences in the estimates exist because: Springer (1988) used daily irradiance data to extrapolate from hourly to daily C fixation rates; our analysis included all stations that fit our

criterion for Shelf water (salinity 31.5-32.7 ppt), including those found within the west bloom; and Springer (1988) estimates were for all regions outside of the west bloom, including Alaskan Coastal water where productivity is low.

Export of Shelf Water Detritus to the Southern Chukchi Sea

The fate of Shelf water primary production south of Bering Strait in 1987 can be ascertained using a simplified daily nitrogen budget analogous to that used for carbon by Walsh (1988). I have estimated an hourly nitrogen productivity rate of $1.34 \text{ mg-at N} \cdot \text{m}^{-2} \cdot \text{h}^{-1}$ for Shelf water in the northeastern Bering Sea. This value can be normalized to a 24 h day for comparison with existing estimates of both grazing (Walsh, 1988) and benthic respiration (Grebmeier, 1987). Consequently, during 15 h of daily primary productivity, a nitrogen productivity rate of $20.1 \text{ mg-at N} \cdot \text{m}^{-2} \cdot \text{d}^{-1}$ is anticipated. Normalization to a 24 h day results in a mean hourly nitrogen productivity rate of $0.84 \text{ mg-at N} \cdot \text{m}^{-2} \cdot \text{h}^{-1}$.

Assuming that pelagic grazers daily consume 30% of local production (inclusive of net zooplankton and microplankton; Walsh, 1988), $0.59 \text{ mg-at N} \cdot \text{m}^{-2} \cdot \text{h}^{-1}$ are available to the detrital pool. Grebmeier (1987) has estimated the average benthic carbon mineralization rate south of Bering Strait (exclusive of Alaskan Coastal water) to be $19.5 \text{ mmol C} \cdot \text{m}^{-2} \cdot \text{d}^{-1}$, which is equivalent to $0.13 \text{ mg-at N} \cdot \text{m}^{-2} \cdot \text{h}^{-1}$ (given a detrital C:N ratio of 6.2; Grebmeier, 1987). With a transfer efficiency of 20% (Walsh, 1988), $0.16 \text{ mg-at N} \cdot \text{m}^{-2} \cdot \text{h}^{-1}$ must be available to support the benthos. In Chapter 1 I estimated that 26% of the daily benthic carbon demand in the northeastern Bering Sea can be met by allochthonous detritus (transported into the ISHTAR area via Anadyr and Shpanberg Straits). The combined rate of transfer to the detrital pool of both allochthonous and autochthonous PN is, then, $0.63 \text{ mg-at N} \cdot \text{m}^{-2} \cdot$

h^{-1} . Since only 25% of this detrital pool is required by the benthos, the remaining 75% could be exported to the Chukchi Sea on a daily basis.

However, the winter nitrogen demands of the benthos must be considered in an annual budget (Fig. 2.9). If summer benthic nitrogen demands are $3.84 \text{ mg-at N} \cdot \text{m}^{-2} \cdot \text{d}^{-1}$ over a 150-day summer season, and consumption is 60% of this value over the remainder of the year (Walsh, 1988), then $1.07 \text{ g-at N} \cdot \text{m}^{-2} \cdot \text{y}^{-1}$ are required by the benthos. Given a nitrogen primary productivity rate of $20.1 \text{ mg-at N} \cdot \text{m}^{-2} \cdot \text{d}^{-1}$ over a 120-day phytoplankton growth season, $2.41 \text{ g-at N} \cdot \text{m}^{-2} \cdot \text{y}^{-1}$ are produced locally and $0.11 \text{ g-at N} \cdot \text{m}^{-2} \cdot \text{y}^{-1}$ are transported into the region, for a total of $2.52 \text{ g-at N} \cdot \text{m}^{-2} \cdot \text{y}^{-1}$ ($181 \text{ g C} \cdot \text{m}^{-2} \cdot \text{y}^{-1}$ assuming a C to N molar ratio of 6). If 30% of the locally produced PN is grazed, and $1.07 \text{ g-at N} \cdot \text{m}^{-2} \cdot \text{y}^{-1}$ are lost to the benthos, then an amount equivalent to 29% of the annual primary production, in addition to 100% of allochthonous material, in Shelf water can be exported to the Chukchi Sea.

Walsh (1988) and Grebmeier (1987) have estimated that 41% and 46%, respectively, of the annual primary production in combined Bering Shelf/Anadyr water is exported from the northeastern Bering Sea while our analysis for Shelf water alone indicates a value of 35% (including allochthonous material). Significantly, their analyses include primary production within Anadyr water (the west bloom), resulting in a greater estimate for annual primary production ($285 \text{ g C} \cdot \text{m}^{-2} \cdot \text{y}^{-1}$).

A separate budget can be established for Anadyr water. The estimate of the average benthic organic carbon mineralization rate for Anadyr/Shelf water ($19.5 \text{ mmol C} \cdot \text{m}^{-2} \cdot \text{d}^{-1}$) is, in fact, weighted to the region overlain by Shelf water since synoptic coverage of the region overlain by Anadyr water is limited by the US:USSR convention line. The distribution of mean benthic organic carbon mineralization rates in the northern Bering Sea (Grebmeier, 1987; her Fig. 4.3) indicates that the position of

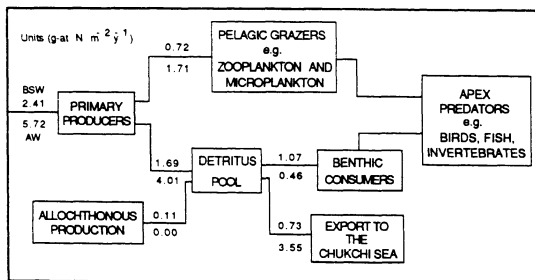


Figure 2.9 An annual nitrogen budget ($\text{g-at N m}^{-2} \text{y}^{-1}$) for modified Bering Shelf water (BSW; top numbers) and Anadyr water (AW; bottom numbers) indicating the fate of nitrogen assimilated by phytoplankton. Nitrogen flux to apex predators was not estimated.

the highest mean values ($40 \text{ mmol C} \cdot \text{m}^{-2} \cdot \text{d}^{-1}$) were located under Shelf water at approximately 65°N and 169°W . Mean mineralization decreases steadily toward the northwest where typical values are $10 \text{ mmol C} \cdot \text{m}^{-2} \cdot \text{d}^{-1}$. It is over this region that the west bloom generally resides.

Mean nitrogen productivity rates in the 1987 west bloom, south of Bering Strait, were $3.18 \text{ mg-at N} \cdot \text{m}^{-2} \cdot \text{h}^{-1}$ (Table 2.1), while Springer (1988) reported mean carbon productivity values in the west bloom of $2.7 \text{ g C} \cdot \text{m}^{-2} \cdot \text{d}^{-1}$ ($324 \text{ g C} \cdot \text{m}^{-2} \cdot \text{y}^{-1}$) for the years 1985-1987. Using the same analysis as for the nitrogen budget in Shelf water (Fig. 2.5; 120 days of phytoplankton growth at 15 hours per day, 150 days of maximal benthic carbon mineralization rates followed by 215 days of mineralization rates reduced by 40%, 20% transfer efficiency in the benthos, and 30% of daily production grazed) I calculate that 62% of the annual primary productivity can be exported to the Chukchi Sea without running down the biological system in the northern Bering Sea. Whereas 29% of the primary productivity in Shelf water was shunted to the benthos, this value is reduced to 8% in Anadyr water. Using the annual carbon primary productivity estimate of Springer (1988), 57% of the production is exported to the Chukchi Sea and 13% is consumed by the benthos.

The actual rate at which PN is transported through Bering Strait into the Chukchi Sea is not known because of limitations in sampling imposed by the US-USSR convention line. However, chlorophyll concentrations of $>1500 \text{ mg} \cdot \text{m}^{-2}$ have been found in the southern Chukchi Sea (Fig. 2.2). These high concentrations are a function of both the plant biomass produced locally in the southern Chukchi Sea and that produced in the northern Bering Sea and transported north through Bering Strait. Springer (1988) has reported high productivity rates in these areas of high plant biomass and, taken together, the phytodetritus available to the pelagic grazers must exceed their capacity

for consumption. Hence, the fate of a large fraction of the primary productivity is the benthos. We now know that 60% of the annual nitrogen-based productivity in Anadyr water is transported into the southern Chukchi Sea where deposition to the sediments may occur. The presence of both anoxic sediments and high organic carbon content in the surface sediments (1.9%) in the region of the chlorophyll bloom (Grebmeier, 1987) lends qualitative support to the analysis.

By determining the fate of nitrogen-based primary productivity in the Anadyr and modified Bering Shelf waters we are able to put some quantitative limits on the transport model presented in Chapter 1. The distribution and fate of plant biomass produced in the two zones of primary productivity of the northern Bering Sea are controlled by strong current fields. Hence, the bulk of the particulate organic material produced in the blooms is not consumed locally but, rather, downstream in current regimes favorable to deposition.

CHAPTER 3: A METHOD FOR ESTIMATING UPTAKE AND PRODUCTION RATES FOR UREA IN SEAWATER USING ^{14}C - AND ^{15}N -UREA

INTRODUCTION

The nitrogen cycle in the marine environment is still far from being fully understood. Several models have been developed that attempt to describe the pathways of the nitrogen nutrients most important to phytoplankton (i.e., nitrate, ammonium, and urea); however, because of methodological problems, the models have not been thoroughly tested.

Urea is an endproduct of heterotrophic nitrogen metabolism that can be utilized by phytoplankton when excreted into aquatic environments. Previous studies of urea utilization by phytoplankton in marine ecosystems (McCarthy, 1972; Harvey and Caperon, 1976; Kristiansen, 1983; Harrison *et al.*, 1985; Price *et al.*, 1985) have been unable to accurately report the rate of urea-N removal from solution and accumulation into the particulate fraction because of the effects of isotope dilution on rate determinations. Further, there has not been a rigorous determination of the urea production rate (Price *et al.*, 1985) other than for individual organisms (Eppley *et al.*, 1973; Smith and Whitledge, 1977), due to an inability to account for isotope dilution of the nutrient tracer (^{15}N -urea) during incubation.

I have developed a method combining ^{14}C -urea and ^{15}N -urea with isotope dilution methods that provides simultaneous estimates of the rates of urea removal from solution (disappearance uptake rates), urea accumulation into the particulate fraction (accumulation uptake rates), and heterotrophic urea production. This method builds upon the work of others in the areas of aquatic nitrogen uptake and remineralization

(Dugdale and Goering, 1967; Blackburn, 1979; Caperon *et al.*, 1979; Gilbert *et al.*, 1982).

Numerous experiments have been performed to determine nitrogen uptake rates. Following the work of Dugdale and Goering (1967) absolute uptake rates (p) were calculated from accumulation of ^{15}N into the particulate fraction:

$$p = (\text{atom } \% \text{ } ^{15}\text{N}_{\text{XS}} \cdot \text{PN}) / R \cdot t \quad (3.1)$$

where $\text{atom } \% \text{ } ^{15}\text{N}_{\text{XS}} = ^{15}\text{N}$ -atom % in the particulate sample adjusted to atom % excess by subtracting the natural abundance of ^{15}N (0.365%), PN = particulate nitrogen content of the sample, R is the ^{15}N -atom % enrichment of the substrate at the beginning of the incubation, and t is the incubation duration. The model assumed a constant ^{15}N -enrichment of the substrate during the incubation. This assumption was made for estimation of nitrogen uptake rates in Chapter 2.

Blackburn (1979) and Caperon *et al.* (1979) developed identical linear differential equation models (here referred to as the Blackburn-Caperon model) for the simultaneous determination of ammonium disappearance and production rates. The Blackburn-Caperon model does not assume a constant value for ^{15}N -enrichment of the substrate and, thus, the initial and final values must be measured. The production rate (D) is calculated as:

$$D = \{[\ln\{(R_t \cdot F)/(R_o \cdot F)\}]/\ln(C_t/C_o)\} \cdot [(C_o - C_t)/t] \quad (3.2)$$

where F is the natural abundance of ^{15}N , C is the substrate concentration, and the subscripts o and t refer to initial and final values. The disappearance uptake rate (U) is calculated as:

$$U = [(C_o - C_t)/t] + D \quad (3.3)$$

Glibert *et al.* (1982) combined the concepts of the Blackburn-Caperon and Dugdale and Goering (1967) models for calculating NH_4^+ uptake and production rates. Accumulation uptake rates were calculated after measuring the accumulation of ^{15}N - NH_4^+ into the particulate fraction and the changes in ^{15}N -enrichment of the NH_4^+ . Laws (1985) presented a formula for calculating accumulation uptake rates (P) that requires determination of the Blackburn-Caperon disappearance uptake rate (U):

$$P = U \cdot (\text{atom } \% \text{ } ^{15}\text{N}_{\text{XS}} \cdot \text{PN}) / (C_o R_o - C_t R_t) \quad (3.4)$$

The Dual-Label Model

The Blackburn-Caperon and Laws (1985) equations have not been used for estimating rates of urea uptake and production because R , the ^{15}N -atom % enrichment of urea, could not be measured. This problem has been overcome by inoculation of samples with both ^{15}N -urea and ^{14}C -urea. The ^{15}N -urea is used in the traditional sense to determine the ^{15}N -atom % excess in the particulate fraction. Because the ^{14}C -urea in solution is removed at the same rate as the ^{15}N -urea (assuming isotopic discrimination is negligible), its activity provides a measure of the quantity of ^{15}N -urea remaining in solution. Determination of the fractional change in ^{14}C -urea

enrichment during the incubation provides a measure of the fractional change in ^{15}N -atom % enrichment.

Enrichment of ^{14}C -urea in water is calculated as:

$$E = A / (V \cdot SA \cdot C) \quad (3.5)$$

where E is the ^{14}C -urea enrichment, A is the activity of the counted sample, V is the volume of the counted sample, SA is the specific activity of the radiolabeled urea, and C is the concentration of urea. From the enrichment of ^{14}C -urea, determined at times T_0 and T_1 , the fractional change (H) in enrichment is calculated as:

$$H = (E_0 - E_1) / E_0 \quad (3.6)$$

where E_0 and E_1 are the initial and final enrichments.

The initial ^{15}N -urea enrichment (R_0) is calculated from the concentration of urea (C_0) determined after the addition of ^{15}N -urea. Thus, C_0 is the sum of ambient and added urea. By calculating R_0 in this way, I have negated the effect of a change in the concentration of urea on the enrichment that may occur in the incubation bottles during the period between the recovery of the water from the collection bottles and the addition of nutrients. Hence:

$$R_0 = [S + [(C_0 - S) \cdot 0.00365] / C_0] \cdot 100 \quad (3.7)$$

where S is the concentration of ^{15}N -urea in the incubation bottle at the start of the

incubation. The final enrichment of ^{15}N -urea (R_t) is calculated as:

$$R_t = R_0 (1 - H). \quad (3.8)$$

Accumulation uptake rates corrected for isotope dilution (P) are calculated according to Equation 3.4. The urea production rate (D) and disappearance uptake rate (U) are calculated from the Blackburn-Caperon model using Equations 3.2 and 3.3, respectively.

METHODS

At two stations in the northeastern Bering Sea, water was collected from the depth of penetration of 50% of the incident photosynthetically active radiation as determined with a Licor LI-185 deck unit and a LI-192S underwater sensor. The water was prefiltered through a 333- μm Nitex® screen into three 2.27-L polycarbonate bottles screened with a neutral density filter (Perforated Products, Inc., nickel screens) to simulate the *in situ* light intensity. Within an hour of sampling the concentration of urea was determined by an automated diacetyl monoxime method (Whitledge *et al.*, 1981), after which 99 atom % ^{15}N -urea (Icon Services, Inc.) was added to each of the samples. The final ^{15}N -atom % enrichment of urea in each sample was less than 5%. In addition, approximately $27 \cdot 10^{-3}$ $\mu\text{g-at}$ urea-N labeled with ^{14}C (1.054 MBq/mg-at urea-N; New England Nuclear Research Products) was added to each of the samples. After mixing, a 125-mL aliquot was removed from each bottle and the remainder was incubated on deck in Plexiglas® incubators cooled with flowing surface seawater.

The 125-mL aliquot was filtered through a 0.6- μm Whatman quartz filter. From the filtrate, triplicate 20-mL aliquots were removed for the determination of the

initial concentration of urea (C_0). To remove ^{14}C - CO_2 produced during urea metabolism, the remaining filtrate (50 - 60 mL) was acidified with 0.5 mL of 1 N HCl and then bubbled with N_2 gas for 15 min. Based on experimentation with ^{14}C - HCO_3^- in the laboratory, this technique removed more than 99% of the dissolved inorganic carbon from solution. To obtain time-zero activity (A_0), 5 mL of the degassed water was added to a scintillation vial containing 15 mL of Scinti Verse I. Counting was performed on a Beckman LS-100C liquid scintillation counter. Twenty-minute counts gave a counting error of 1-1.5%.

Samples were incubated for 6-8 h. Prior to filtration, a 125-mL aliquot was removed and treated as at T_0 to determine the concentration of urea (C_t) and the activity of ^{14}C -urea (A_t). The remaining 2.02 L was filtered onto a precombusted (450°C) 0.6- μm quartz filter and rinsed with filtered seawater. Filter preparation for isotope ratio analysis and particulate nitrogen determination is described in Chapter 2.

At an additional station (Station 3093), the particulate phase was size-fractionated to evaluate better the fate of the ^{15}N -urea. Prior to incubation, water was passed through 202- μm or 20- μm Nitex® screens or a 3.0- μm Nuclepore polycarbonate membrane. The chlorophyll *a* concentration of each fraction was determined by fluorometry (Parsons *et al.*, 1984) using a Turner Designs Model 10 fluorometer.

RESULTS AND DISCUSSION

Accumulation uptake rates (Table 3.1), uncorrected for isotope dilution (p), were calculated with R_0 (in excess of natural abundance) using Equation 3.1. Estimates of uptake rates, when corrected for isotope dilution, were increased by averages of 25% and 83% (Stations 2101 and 2120, respectively) with the accumulation model (Equation 3.4) and by averages of 265% and 210% (Stations 2101 and 2120,

Table 3.1 Absolute uptake rate of urea without correction for isotope dilution (p) and with correction (P - accumulation uptake rate; U - disappearance uptake rate) and production rates (D). Sample are replicated with seawater from the 50% light depth at two stations in the northeastern Bering Sea. S is the concentration of ^{15}N -urea (exclusive of naturally occurring ^{15}N -urea) at the start of the incubation, C is the concentration of dissolved urea, R is the ^{15}N -urea enrichment (%), A is the ^{14}C -urea activity, E is the ^{14}C -urea enrichment, H is the fractional change in enrichment, and PN is the particulate nitrogen concentration. Subscripts 0 and 1 refer to initial and final incubation times. Units for S , C_0 , C_1 , and PN are $\mu\text{g-at N L}^{-1}$, those of A_0 and A_1 are Bq, and those of p , P , U , and D are $\mu\text{g-at N L}^{-1} \text{ h}^{-1}$. Standard deviations are in parentheses.

Replicate	S	C_0	R_0	A_0	E_0	C_1	A_1	E_1	H	R_1	$A_1 \times 8$	Incubation Time (h)	PN	p	P	U	D
Station No. 2101																	
1	0.009	0.529 (0.115)	2.060	52.540	18.846	0.389 (0.014)	25.456	12.417	0.341	1.357	0.093	6.610	2.119	0.019	0.022	0.063	0.040
2	0.009	0.713 (0.084)	1.623	44.733	11.905	0.433 (0.123)	20.054	8.788	0.262	1.198	0.100	6.160	1.969	0.025	0.025	0.082	0.037
3	0.009	0.473 (0.062)	2.261	50.542	20.276	0.481 (0.180)	24.975	9.852	0.514	1.099	0.097	6.160	2.051	0.017	0.027 $x=0.025$ (0.002)	0.074 $x=0.073$ (0.009)	0.073 $x=0.050$ (0.020)
Station No. 2120																	
1	0.022	0.552 (0.008)	4.336	55.981	19.243	0.595 (0.012)	20.165	6.431	0.666	1.448	0.608	7.500	1.725	0.035	0.067	0.098	0.104
2	0.022	0.508 (0.023)	4.680	51.800	19.349	0.578 (0.006)	21.904	7.191	0.628	1.741	0.485	7.500	1.099	0.016	0.028	0.071	0.080
3	0.022	0.579 (0.005)	4.151	43.475	14.248	0.633 (0.004)	15.059	4.514	0.683	1.315	0.609	7.500	1.680	0.036	0.066 $x=0.054$ (0.022)	0.102 $x=0.090$ (0.017)	0.109 $x=0.098$ (0.015)

respectively) with the disappearance model (Equation 3.3). The large coefficient of variation (CV) associated with replicate estimates of accumulation rates from Station 2120 (41%) was caused by an anomalously low PN and atom % excess in replicate 2. Replicates 1 and 3 are in very good agreement, with a CV of <0.1%. Station 2101 exhibited a CV of 8% for accumulation uptake rates. Coefficients of variation for urea production rates were 15% and 40% for Stations 2120 and 2101, respectively.

The ^{15}N data was evaluated for mass balance using ^{14}C activity in the aqueous phase as an indication of ^{15}N -urea remaining in solution. The ^{15}N that had disappeared from the dissolved ^{15}N -urea pool was consistently greater than the amount of ^{15}N that had accumulated in the particulate fraction (Table 3.2). On average, 58% (Station 2101) and 37% (Station 2120) of ^{15}N -urea removed from solution could not be accounted for in the particulate phase. The missing ^{15}N may have accumulated as ^{15}N -labeled dissolved organic nitrogen (DON) or NH_4^+ . Possible avenues include phytoplankton leakage and grazer-induced losses, such as zooplankton excretion, leakage, and loss of soluble plant material at the mouth parts.

Observations of dissolved inorganic nitrogen disappearance in excess of particulate nitrogen accumulation are not new. Dugdale and Wilkerson (1986) found that 66% of the disappearance of NH_4^+ and 76% of the disappearance of NO_3^- at the 50% light penetration depth off Peru was accounted for by ^{15}N accumulation in the particulate fraction. Price *et al.* (1985) reported that the change in concentration of dissolved inorganic nitrogen and urea was consistently greater than the change in PN in frontal waters off British Columbia.

To further evaluate the apparent loss of ^{15}N from the particulate phase, particulate material was size fractionated and, following incubation, the resulting ^{15}N distribution evaluated (Table 3.2). Although the <20- μm fraction had only a 4%

Table 3.2 Fraction of ^{15}N -urea removed from the dissolved phase which is unaccounted for in the particulate phase (FR). Stations 2101 and 2120 are replicated at one depth while Station 3039 is size fractionated (<200, <20, and <3 μm). S_0 and S_t are the initial and final concentrations ($\mu\text{g-at N L}^{-1}$) of ^{15}N -urea. S_t is estimated from the fractional reduction in ^{14}C -urea activity. Initial (A_0) and final (A_t) ^{14}C -urea activities are expressed in Bq. $^{15}\text{N}_{\text{XS}}$ is the ratio of ^{15}N to total N in the particulate phase (minus 0.00367). PN is the particulate nitrogen concentration ($\mu\text{g-at N L}^{-1}$). Chl is the chlorophyll *a* concentration ($\mu\text{g L}^{-1}$). FR is calculated as $[(S_0 - S_t) - (^{15}\text{N}_{\text{XS}} \cdot \text{PN})] \cdot [(S_0 - S_t)]^{-1}$.

Replicate	S_0	$(A_0 - A_t) \cdot A_0^{-1}$	S_t	$^{15}\text{N}_{\text{XS}}$	PN	$^{15}\text{N}_{\text{XS}} \cdot \text{PN}$	FR	Chl
Station No. 2101								
1	0.009	0.515	0.0044	0.00093	2.119	0.00197	0.57	-
2	0.009	0.552	0.0040	0.00100	1.969	0.00197	0.61	-
3	0.009	0.506	0.0044	0.00097	2.051	0.00199	0.57	-
Station No. 2120								
1	0.022	0.640	0.0079	0.00608	1.725	0.0105	0.25	-
2	0.022	0.577	0.0093	0.00485	1.099	0.0053	0.58	-
3	0.022	0.653	0.0076	0.00609	1.680	0.0102	0.29	-
Station No. 3039								
<200	0.009	0.443	0.0050	0.00072	3.37	0.0024	0.40	3.08
<20	0.009	0.103	0.0081	0.00040	2.13	0.0008	0.11	2.95
<3	0.009	0.087	0.0082	0.00028	2.49	0.0007	0.12	2.06

reduction in chlorophyll *a* concentration relative to the <200- μm fraction, there was a 72% improvement in our ability to account for ^{15}N removed from solution as ^{15}N -urea. A 33% reduction in the concentration of chlorophyll *a* (<3- μm fraction) provided no further improvement in the recovery of ^{15}N . These results point to the importance of the >20- μm fraction in effecting the loss of ^{15}N . Perhaps large-celled phytoplankton (>20- μm) are especially prone to leak DON and NH_4^+ , or microzooplankton (>20- μm) play a significant role in causing a grazer-induced loss of nitrogen from the plant cells.

Filtration through the 20- μm screen reduced the concentration of PN by 37%. Much of the PN removed must be detrital; however, a portion also must be composed of microzooplankton and the removal of these grazers improved the nitrogen retention efficiency of the phytoplankton. The removal of the nanoplankton fraction (3-20 μm) provided no further improvement in recovery of ^{15}N , suggesting that the mechanism controlling the retention of urea-N in the <20- μm size class is common throughout that size class. Possible mechanisms for the apparent loss of ^{15}N from the <20 μm fraction include: grazer-induced and self-induced leakage of ^{15}N as DON and NH_4^+ by the plant cells, analytical errors, and fractionation of ^{14}C - and ^{15}N -urea during uptake (thus providing an error in my estimates of the remaining pool of dissolved ^{15}N -urea). I am confident in my analytical ability to precisely measure the ^{15}N atom % excess of the PN, the nitrogen content of the PN, and the ^{14}C activity of the aqueous phase. These measurements, and a knowledge of the initial concentration of ^{15}N -urea, provide the only values required for this mass balance analysis. Whereas some fractionation of ^{14}C - and ^{15}N -urea during uptake must exist, I doubt that it could be responsible for the noteworthy lack of accountability of ^{15}N . This argument is supported by noting the improved accountability of ^{15}N in the <20- μm fraction, which still contained 96% of the concentration of chlorophyll *a*, over that of the <200- μm fraction.

Plant- and grazer-induced leakage is, then, the most likely cause for loss of ^{15}N in the $<20\text{-}\mu\text{m}$ size class. Plant-induced leakage must account for the bulk of the 11-12% of ^{15}N removed from the urea pool that could not be accounted for in the $<20\text{-}\mu\text{m}$ and $<3\text{-}\mu\text{m}$ particulate phases (Table 3.2) because there was no improvement in ^{15}N recovery in the $<3\text{-}\mu\text{m}$ size class relative to the $<20\text{-}\mu\text{m}$ fraction, while there must have been a reduction in the grazing stress following this fractionation.

In the $<200\text{-}\mu\text{m}$ samples, 40% of the ^{15}N removed from solution as urea could not be accounted for in the particulate pool. If we extend the approximate 10% loss due to plant leakage in the $<20\text{-}\mu\text{m}$ fraction to the entire $<200\text{-}\mu\text{m}$ plant population, the remaining 30% loss can be attributed to grazing stress. This implies that most of the assimilated urea-N is going into a persistent soluble pool, which only slowly goes to a particulate form. The soluble pool is readily lost during grazing.

Glibert *et al.* (1985), in discussing the implications of missing ^{15}N , suggested that it is important to determine whether the uptake of nitrogen by phytoplankton is reported more accurately by the disappearance of ^{15}N from the dissolved phase or by the accumulation of ^{15}N in the particulate phase. This is a distinction between gross and net nitrogen uptake by the phytoplankton if we can attribute most of the urea removal to plant cells. Plants probably play the most significant role in urea consumption since bacterial utilization of urea is not thought to occur at significant rates in oceanic water (Wheeler and Kirchman, 1986) and it is unlikely that abiotic pathways for loss of urea are important. As seen here, the difference between the disappearance and accumulation uptake rates can provide insight to the relative importance of plant- and grazer-induced loss of nitrogen.

This method is, in fact, subject to underestimates of the amount of ^{15}N missing from the combined pool of particulate nitrogen and urea nitrogen. ^{14}C -labeled dissolved

organic carbon (DOC) may be released into the water, causing an overestimate of the amount of ^{15}N -urea in solution. If this process is important for the autotrophs in the $<20\text{-}\mu\text{m}$ fraction, the apparent improvement in accountability of ^{15}N would be misleading. In other high latitude waters, $<10\%$ of the urea-C taken up by the plants was incorporated into particulate matter, with the rest disposed of as $^{14}\text{C-CO}_2$ (Harrison *et al.*, 1985). During the incubations, approximately 50% of the ^{14}C -urea was removed from solution. If we assume that 10% of this carbon is incorporated into the organic fraction and that 50% of the assimilated carbon is lost as DOC, then 2.5% of the ^{14}C initially in solution would be returned as $^{14}\text{C-DOC}$. The $^{14}\text{C-DOC}$ returned would cause a 4% underestimate of the amount of ^{15}N missing from the pool of particulate nitrogen and dissolved urea. Using data from Station 2101 (replicate 1) and assuming that 2.5% of the urea carbon removed from solution is reintroduced as $^{14}\text{C-DOC}$, I calculate that the accumulation and disappearance uptake rates of urea-N would be underestimated by 2.7% and 5.5% and that the production rate of urea-N would be underestimated by 6.3%.

Calculating urea uptake rates based on rates of disappearance provides values that average 140% greater than those calculated for rates of accumulation for northeastern Bering Sea data. Glibert *et al.* (1982) presented data (their Tables 2 and 3) where ammonium disappearance uptake rates exceeded accumulation uptake rates by an average of 197%. The ratio of the rate of urea production to the rate of urea uptake is also greatly affected by the model used for calculation of uptake rates. For Station 2120, the production:uptake ratios are 1.8 and 1.1, respectively, for the accumulation and disappearance models.

My results show that the *in situ* production of urea is approximately equal to the consumption of urea (i.e., dynamic steady state) and that a portion of the urea-N that is

consumed must be remineralized quickly. The data suggest that to describe more completely the cycling of urea-N, models must include a dissolved organic pool, as has been recognized for NH_4^+ (LaRoche and Harrison, 1987).

Prior studies of the uptake of urea by phytoplankton have not accounted for isotope dilution during incubation. Studies of urea regeneration have been limited in the same way and have depended on mass balances and determinations of uptake rates uncorrected for isotope dilution. This method provides improved and direct estimates of *in situ* urea production and uptake rates. Trace addition of labeled substrate is achievable with this method and, as a consequence, changes in substrate concentration and fluxes are not significant. The method is performed with relative ease in fresh or marine water and requires minimal effort beyond that needed for conventional uptake experiments which do not account for isotope dilution.

CHAPTER 4: SUMMARY AND CONCLUSIONS

The primary intent of Chapters 1 and 2 is to describe the geographical distribution and fate of primary productivity over the Bering Sea shelf in summer. By considering the nutrient content and advective nature of the water masses in the region, we can begin to understand the forces controlling these characteristics of primary productivity in this rich ecosystem.

In Chapter 1, a descriptive model for summer primary production and consumption on the northern Bering Sea shelf is proposed. There are two important regions for primary production over the shelf: the first has its beginnings over the shelf break and the other in the western portion of the Chirikov Basin. Both regions are strongly advected; hence, the effect of this primary productivity on higher trophic levels extends over a large area. These two regions of productivity are wholly dependent on the flux of nutrients, and nitrate in particular, from deeper water comprising the Bering Slope/Anadyr Currents into outer domain/modified Bering Shelf water.

Based on data from both the PROBES and ISHTAR projects, I conclude that production at the shelf break front is initiated in May, when water column stability favors plant growth, and continues into the fall, when frequent wind mixing of the surface water column and declining day lengths result in reduced net plant productivity. Productivity associated with the shelf break front is estimated to be $200 \text{ g C} \cdot \text{m}^{-2}$ over the 120-day growing period. Near-bottom chlorophyll *a* concentrations are $<1 \text{ mg} \cdot \text{m}^{-3}$ and sinking rates of phytoplankton are estimated to be $1 \text{ m} \cdot \text{d}^{-1}$ at the shelf break front (Iverson *et al.*, 1979b). Consequently, shelf break production is diverted directly to the pelagic food web of the outer shelf domain throughout summer.

The Bering Slope Current bifurcates at Cape Navarin and the northern branch, now referred to as the Anadyr Current, crosses the Gulf of Anadyr and passes through Anadyr and Bering Straits. I interpret the data to indicate that the system of plant biomass production located above the shelf break front is deflected to the north with the Anadyr Current and, as part of the

modified Bering Shelf water mass, bifurcates at St. Lawrence Island. This process explains the presence of a deep layer of phytoplankton to the east and west of St. Lawrence Island and north of the island throughout the summer. The phytodetritus transported around St. Lawrence Island supplies 26% of the daily carbon demand of the rich amphipod beds located in the Chirikov Basin, south of Bering Strait. We have known that secondary production over the outer shelf is predominantly pelagic while that in the Chirikov Basin is benthic. However, the data supports the conclusion that it is the same system of primary productivity that sustains these spatially distinct pelagic and benthic consumers. During shoaling of modified Bering Shelf water from the shelf break (200 m) to Chirikov Basin (<50 m), a transition is made from a predominantly pelagic food web to one that is directly tied to the benthos.

Malone *et al.* (1983) described a similar production and transport process at the shelf break of the New York Bight. They found that development of stratification in nutrient-rich offshore water between storm events results in high growth rates and biomass near the surface on the shelf side of the shelf break front. During the summer, as is the case at the Bering Sea shelf break, plant growth occurred at the pycnocline. Unlike the Bering Sea, however, where transport is from the shelf break front to the inner shelf, up to 35% of annual production over the continental shelf of the New York Bight is exported from shelf to slope water.

This comparison highlights the unusual nature of the ecosystem in the northern Bering Sea. The transport of nutrient-rich water from depth at the outer shelf to the inner shelf, resulting in an intense phytoplankton bloom throughout the summer, is a feature of shelf circulation unique to the Bering Sea. Transport from outer- to inner-shelf exists because of the breach between the North American and Asian land masses (Bering Strait) and the orientation of the regional wind regime, which drives the flow to the north (Coachman *et al.*, 1975). The onshelf intrusion of nutrient-rich slope water for most shelves occurs at the wind-event, eddy, and diffusive time scales (Walsh, 1988). Of these, the eddy transport of nutrient-rich water over long

distances, like that for Gulf Stream eddy-induced water exchange in the the mid-Atlantic Bight (Morgan and Bishop, 1977), is the most comparable to the advection found in the northern Bering Sea.

The Anadyr Current, meanwhile, shoals at the shallow Anadyr Strait creating a second region of productivity. An intense surface bloom (the west bloom) develops north of Anadyr Strait as a result of the sudden influx of nitrate to the euphotic zone. The west bloom is strongly advected to the north through Bering Strait, where it is joined by the east bloom, ultimately to be deposited in the sediments of the southern Chukchi Sea. The bloom, once north of Bering Strait and in the southern Chukchi Sea, is part of a relatively weak current system. Reduced current speed results in reduced bathymetric mixing of the water column, resulting in increased sedimentation rates and deposition of phytodetritus. As a result, large amounts of organic material settle to the sediment to support a rich benthos and large populations of the organisms supported by that benthos (e.g., marine mammals).

In Chapter 2, some quantitative limits are put on the production and transport of plant material in the Anadyr and modified Bering Shelf water masses. To determine the fate of the plant biomass produced, nitrogen-based productivity rates were first determined. Where nutrient-rich Anadyr water was well-mixed to near-surface, and no surface accumulation of chlorophyll was evident (as is commonly found immediately north of Anadyr Strait), total nitrogen (nitrate, ammonium, and urea combined) productivity rates were $<1.4 \text{ mg-at N} \cdot \text{m}^{-2} \cdot \text{h}^{-1}$. Nitrate-based productivity represented $>60\%$ of total nitrogen uptake on average and, at one station, was 80% . Synoptic collection of data in the highly productive west bloom was prevented by the US-USSR convention line. However, nitrogen productivity measured in the bloom was, on average, 3.18 and $6.11 \text{ mg-at N} \cdot \text{m}^{-2} \cdot \text{h}^{-1}$ south and north of Bering Strait, respectively. Nitrate-based productivity averaged $<50\%$ of total nitrogen uptake in the west bloom. Total nitrogen productivity rates in modified Bering Shelf water were approximately 70% greater than those

measured in prebloom Anadyr water, reflecting both higher specific uptake rates and greater particulate nitrogen concentrations, while the contribution of nitrate to the total nitrogen consumed was halved from 64% in Anadyr water to 26.8%. East bloom productivity rates were of the same magnitude as the remainder of the modified Bering Shelf water.

A simple nitrogen budget was constructed to estimate the fraction of total annual production in the Anadyr and modified Bering Shelf water masses that can be exported north through Bering Strait for deposit in the benthos of the southern Chukchi Sea. Based on nitrogen productivity rates presented here, and existing estimates of both grazing and benthic respiration, 62% and 29% of the annual primary production in Anadyr and Shelf waters, respectively, can be exported to the Chukchi Sea without "running down" the biological system in the northern Bering Sea. These results confirm the important role that advection plays in dictating the fate of phytodetritus as hypothesized in Chapter 1.

The actual rate at which phytodetritus is transported through Bering Strait into the Chukchi Sea is not known; however, both anoxic sediments and surface sediments with high organic carbon content have been reported to exist in the southern Chukchi Sea. Walsh (1988) and Grebmeier (1987) have estimated that 41% and 46%, respectively, of the annual primary production in combined Bering Shelf/Anadyr water is exported from the northeastern Bering Sea. It is not surprising that their estimates for the combined water masses fall between my estimates for the individual water masses.

It is clear that, quantitatively, deposition of phytodetritus is the most important fate of the plant material produced in the northern Bering Sea. Without continual resuspension of the phytoplankton cells from both wind and bathymetric mixing the plant cells are bound to fall to the sediments. Wind mixing in the northern Bering Sea is important to that portion of the water column above the pycnocline while bathymetric mixing is important below the pycnocline. The west bloom, a surface phenomenon, is suspended by wind mixing. As the bloom passes through

Bering Strait the water column is well-mixed and suspension becomes a function of bathymetric mixing, which in turn is a function of current speed. Current speed is greatly reduced in the southern Chukchi Sea and deposition occurs. The deep chlorophyll layer of the modified Bering Shelf water, on the other hand, enters the ISHTAR area below the pycnocline. Mixing occurs through Shpanberg and Anadyr Straits and deposition follows the reduction of current speed in the Chirikov Basin.

In other upwelling systems, such as off the Oregon coast, the fate of phytodetritus is consumption by grazers. Suspension of the plant cells continues to be a function of the wind, as is the upwelling event itself. The winds continue from late March into October (Walsh, 1988) and most plant cells remain in suspension until grazed by the zooplankton. As the bloom moves offshore, the depth of the water column becomes greater and the chance of a cell falling to the sediments without being grazed becomes smaller.

Because nutrient input to the northern Bering Sea is a summer-long upwelling event, primary productivity is maintained at high levels for long periods of time. The physical processes that maintain primary productivity throughout the summer in the Anadyr water of the northern Bering Sea are analogous to those processes associated with a continuous culture system. Nutrient-rich water enters the system via Anadyr Strait and, as reflected in the west bloom, the phytoplankton community responds with rapid and sustained growth. Meanwhile, plant material and unused nutrients are removed from the system through Bering Strait.

The natural environment is not as simplistic as the chemostat analogy may suggest. In the sea, nitrate supports the exponential growth phase of bloom development while regenerated nitrogen maintains the growth at high levels. Likewise, in the region of the west bloom, nitrate is the nutrient of importance during bloom development. However, plant population increases are greatly enhanced by stabilization of the water column and stabilization is characteristic of a layered water column. As a result, where plant growth is maximal a vertical gradient in the concentration

of nitrate exists, with high concentrations at depth where little plant growth occurs and low concentrations at the surface where plant growth is the greatest. When this concentration gradient develops, utilization of nitrate by the plant cells is limited by diffusion of the nutrient into the surface layer. On the contrary, regenerated nutrients are produced in the water layer in which the phytoplankton reside so the use of these nutrients is favored by, among other factors, availability. These observations are supported by the sequence of nutrient preference during bloom development and maintenance in the northern Bering Sea.

Interesting follow-up studies could be performed both upstream and downstream of the ISHTAR study area given approval to work in Soviet waters. We know that the Anadyr Current carries with it the nitrate necessary to sustain the west bloom. If the Anadyr Current was slowed or deflected from its current path there could be vast changes in the ecosystem of the northern Bering Sea. This would have major implications for all consumers in the area. As discussed, the source of the Anadyr Current is the Bering Slope Current and its bifurcation at Cape Navarin. If the bifurcation were to be displaced further south of Cape Navarin, it may be that a larger proportion of the Bering Slope Current would flow south and transport within the Anadyr Current would be reduced. Reversals of flow in Bering Strait may play a role in determining the position of the bifurcation simply by causing the current regime in the northern Bering Sea to back up or be deflected. We need to understand the mechanisms that control production of the Anadyr Current.

Another appropriate study would be to determine the distribution and fate of primary productivity in the western Chukchi Sea. Based on limited CZCS imagery available for the southern Chukchi Sea, I believe that the majority of primary productivity in that region takes place in Soviet waters. In fact, the productivity occurring west of the convention line is likely greater than any productivity measured in American waters as part of the ISHTAR project. It would be very interesting to determine whether this is true and to determine what fraction of the nitrate

associated with the Anadyr Current is consumed in the southern Chukchi Sea and how much passes unused into the Arctic Ocean.

The objective of Chapter 3 was to describe a method that would allow a direct measure of the rates of autotrophic uptake and heterotrophic production of urea. Though it may be an artifact imposed by existing detection limits, this nutrient has been considered more important in coastal than oceanic waters. Accordingly, urea proved prominent in the northern Bering and southern Chukchi Seas where its average contribution to total nitrogen productivity ranged from 15-41%.

Previously, there had not been a rigorous determination of urea production or uptake rates due to an inability to account for isotope dilution of the nutrient tracer (^{15}N) during incubation. As a result, reports of urea uptake rates have been underestimated when any significant urea production has taken place concurrently. Improved estimates of the rates of urea production and uptake by phytoplankton in the northern Bering Sea were made after determining the change in ^{15}N -atom % enrichment of urea during incubations. A method is described by which the change in enrichment is measured using ^{14}C -urea to trace the ^{15}N -urea in solution. Estimates of uptake rates are increased (relative to uptake rates determined without correction for isotope dilution) by up to 83% using a ^{15}N accumulation model and by >210% using a ^{15}N disappearance model.

A discrepancy was found to exist between ^{15}N -urea removed from the aqueous phase and ^{15}N accumulated in the particulate phase. The ability to find in the particulate fraction the ^{15}N removed from solution as ^{15}N -urea was improved by 72% following removal of the >20- μm particulate fraction. This corresponded to only a 4% reduction in the concentration of chlorophyll *a* and a 37% reduction in the concentration of particulate nitrogen. These results suggest that the removal of microzooplankton may have improved the efficiency of urea-N retention by phytoplankton. If microzooplankton are implicated as the causative agents, the method may offer an alternative means by which grazing stress can be assessed.

Springer (1988) has estimated annual primary production in the west bloom of the northern Bering Sea to be greater than $300 \text{ g C} \cdot \text{m}^{-2} \cdot \text{y}^{-1}$. Except for the major upwelling regions associated with the eastern boundary currents off Peru and southwest Africa, this productivity is comparable to, or greater than, existing estimates from the world's shelf regions evaluated to date (Walsh, 1988). The most important factor limiting annual productivity is probably the length of the growing season at this high latitude. In the spring, wind mixing of the water column prevents significant plant growth where open water exists. Sea ice further limits the amount of light penetrating the water column. In the fall, day length decreases rapidly bringing the season of productivity to a close. This is in contrast to the major upwelling regimes nearer the equator where long days provide adequate light and productivity is limited by nutrient availability and grazing.

The fate of primary production in the northern Bering and southern Chukchi Seas is the sediment and several large populations of organisms, including man, are dependent on this aspect of the ecosystem. As of this writing, anthropogenic impact is not evident in the northern Bering Sea and the system studied by the ISHTAR program remains in a relatively pristine state. However, the worst oil spill in the history of this nation occurred this year in Prince William Sound, Alaska and its long-term effects are uncertain. On the short-term, many species of marine organisms have suffered greatly and many human livelihoods have been disrupted. Oil drilling is anticipated in Bristol Bay of the southeastern Bering Sea and, given the model proposed for primary production and transport in the area, we can try to estimate the impact of a major oil spill in the region. If a spill occurred during larval development of the commercially important fish species, as apparently has happened in Prince William Sound, several years of catch could be eliminated. As oil moves downstream with the currents, it could eventually be deposited in the sediments of the Chirikov Basin or the southern Chukchi Sea. This would certainly affect the benthos and all organisms dependent upon it. Marine birds, mammals and, finally, the

indigenous human populations would be severely impacted. Perhaps our recently developed comprehension of Bering Sea ecosystem processes will be useful to policy makers weighing the risks of oil field development on the Bering Sea shelf.

References

- Aagaard K., A. T. Roach and J. D. Schumacher (1985) On the wind-driven variability of the flow through Bering Strait. *Journal of Geophysical Research* **90**, 7213-7221.
- Bidigare R. R. (1983) Nitrogen excretion by marine zooplankton. In: *Nitrogen in the Marine Environment*, E. J. Carpenter and D G. Capone, eds., Academic Press, pp. 385-410.
- Blackburn T. H. (1979) Method for measuring rates of NH_4^+ turnover in anoxic marine sediments, using a ^{15}N - NH_4^+ dilution technique. *Applied Environmental Microbiology* **37**, 760-765.
- Caperon J., D. Schell, J. Hirota and E. Laws (1979) Ammonium excretion rates in Kaneohe Bay, Hawaii, measured by a ^{15}N isotope dilution technique. *Marine Biology* **54**, 33-40.
- Coachman L. K. (1986) Circulation, water masses, and fluxes on the southeastern Bering Sea shelf. *Continental Shelf Research* **5**, 23-108.
- Coachman L. K. and K. Aagaard (1988) Transports through Bering Strait: annual and interannual variability. *Journal of Geophysical Research* **93**, 15535-15539.
- Coachman L. K., K. Aagaard and R. B. Tripp (1975) *Bering Strait: the regional physical oceanography*, University of Washington Press, Seattle, Washington, 172 pp.
- Coachman L. K., T. H. Kinder, J. D. Schumacher and R. B. Tripp (1980) Frontal systems of the southeastern Bering Sea shelf. In: *Second International Symposium on Stratified Flows*, Vol. 2, T. Carstens and T. McClimans, eds., Trondheim, pp. 917-933.

- Coachman L. K. and J. J. Walsh (1981) A diffusion model of cross-shelf exchange of nutrients in the Bering Sea. *Deep-Sea Research* **28**, 819-837.
- Cochlan W. P. (1986) Seasonal study of uptake and regeneration of nitrogen on the Scotian Shelf. *Continental Shelf Research* **5**, 555-577.
- Dudek N., M. A. Brzezinski and P. A. Wheeler (1986) Recovery of ammonium nitrogen by solvent extraction for the determination of relative ^{15}N abundance in regeneration experiments. *Marine Chemistry* **18**, 59-69.
- Dugdale R. C. and J. J. Goering (1967) Uptake of new and regenerated forms of nitrogen in primary productivity. *Limnology and Oceanography* **12**, 196-206.
- Dugdale R. C. and F. P. Wilkerson (1986) The use of ^{15}N to measure nitrogen uptake in eutrophic oceans; experimental considerations. *Limnology and Oceanography* **31**, 673-700.
- Eppley R. W., E. H. Renger, E. L. Venrick and M. M. Mullin (1973) A study of plankton dynamics and nutrient cycling in the central gyre of the north Pacific Ocean. *Limnology and Oceanography* **18**, 534-551.
- Fisher T. R. and K. M. Morrissey (1985) A new method for the recovery of ammonium from natural waters for measurement of ^{15}N composition in isotope dilution experiments. *Marine Chemistry* **16**, 11-21.
- Glibert P. M., F. Lipshultz, J. J. McCarthy and M. A. Altabet (1982) Isotope dilution models of uptake and remineralization of ammonium by marine plankton. *Limnology and Oceanography* **27**, 639-650.
- Glibert P. M., F. Lipshultz, J. J. McCarthy and M. A. Altabet (1985) Has the mystery of the vanishing ^{15}N in isotope dilution experiments been resolved? *Limnology and Oceanography* **30**, 444-447.

- Goering J. J. and R. L. Iverson (1978) Primary Production and Phytoplankton Composition. PROBES Phase I Progress Report 1977-1978, University of Alaska, Fairbanks, Alaska, 488 pp.
- Gottschalk G. (1986) *Bacterial Metabolism*. Springer-Verlag, 2nd ed., 359 p.
- Grebmeier J. M. (1987) The ecology of benthic carbon cycling in the northern Bering and Chukchi Seas. Ph.D. Dissertation, Univ. Alaska, Fairbanks, 189 pp.
- Harrison W. G., E. J. Head, R. J. Conover, A. R. Longhurst and D. D. Sameoto (1985) The distribution and metabolism of urea in the eastern Canadian Arctic. *Deep-Sea Research* **32**, 23-42.
- Harvey, W. A. and J. Caperon. (1976) Rate of utilization of urea, ammonium, and nitrate by natural populations of marine phytoplankton in an eutrophic environment. *Pacific Science* **30**, 329-340.
- Hattori A. and E. Wada. (1974) Assimilation and oxidation-reduction of inorganic nitrogen in the North Pacific Ocean. In: *Oceanography of the Bering Sea with emphasis on renewable resources*, D. W. Hood and E. J. Kelly, editors, Vail-Baillou Press, pp. 149-162.
- Hufford G. L. and D. M. Husby (1970) Oceanographic survey of the Gulf of Anadyr, 2-16 August 1970. U.S. Coast Guard Oceanographic. Rep. No. 52, CG 373-52, Washington, D.C., 52 pp.
- Inner Shelf Transfer and Recycling (1985) ISHTAR Data Report No. 1, 1985 Hydrographic Data, STD, Nutrients, & Chlorophyll. Institute of Marine Science, University of Alaska, Fairbanks, Alaska.
- Inner Shelf Transfer and Recycling (1987) ISHTAR Data Report No. 9, 1987 Hydrographic Data, STD, Nutrients, & Chlorophyll. Institute of Marine Science, University of Alaska, Fairbanks, Alaska.

- Iverson R. L., L. K. Coachman, R. T. Cooney, T. S. English, J. J. Goering, G. L. Hunt, Jr., M. C. Macauley, C. P. McRoy, W. S. Reeburgh and T. E. Whittedge (1979a) Ecological significance of fronts in the southeastern Bering Sea. In: *Ecological Processes in Coastal and Marine Systems*, R. J. Livingston, editor, Plenum Press, New York, pp. 437-466.
- Iverson R. L., T. E. Whittedge and J. J. Goering (1979b) Chlorophyll and nitrate fine structure in the southeastern Bering Sea shelf break front. *Nature, London*, **281**, 664-666.
- Kinder T. H., D. C. Chapman and J. A. Whitehead, Jr. (1986) Westward intensification of the mean circulation on the Bering Sea shelf. *Journal of Physical Oceanography* **16**, 1217-1229.
- Kinder T. H. and L. K. Coachman (1978) The front overlaying the continental slope in the eastern Bering Sea. *Journal of Geophysical Research* **83**, 4551-4558.
- Kristiansen S. (1983) Urea as a nitrogen source for phytoplankton in the Oslofjord. *Marine Biology* **74**, 17-24.
- LaRoche J. and W. G. Harrison (1987) Compartmental models of nitrogen cycling in tropical and temperate marine environments. *Marine Ecology-Progress Series* **38**, 137-149.
- Laws E. A. (1985) Analytic models of NH_4^+ uptake and regeneration experiments. *Limnology and Oceanography* **30**, 1340-1350.
- Lipshultz F., S. C. Wofsy and L. E. Fox (1986) Nitrogen metabolism of the eutrophic Delaware River ecosystem. *Limnology and Oceanography* **31**, 701-716.
- Malone T. C., T. S. Hopkins, P. G. Falkowski and T. E. Whittedge (1983) Production and transport of phytoplankton biomass over the continental shelf of the New York Bight. *Continental Shelf Research* **1**, 305-337.

- McCarthy J. J. (1972) The uptake of urea by natural populations of marine phytoplankton. *Limnology and Oceanography* **17**, 738-748.
- McRoy C. P. (1983) Cruise Report, R/V Alpha Helix 049, 15-26 August 1983, University of Alaska Fairbanks, Fairbanks, Alaska.
- McRoy C. P. and J. J. Goering (1974) The influence of ice on the primary productivity of the Bering Sea. In: *Oceanography of the Bering Sea*, D. W. Hood and E. J. Kelly, editors, Occasional Publication No. 2, Institute of Marine Science, Univ. of Alaska, Fairbanks, pp. 403-421.
- McRoy C. P., J. J. Goering and W. E. Shiels (1972) Studies of primary production in the eastern Bering Sea. In: *Biological oceanography of the northern north Pacific Ocean*, A. Y. Takenouti, Ed., Motoda Commemorative Vol. 3, Idemitsu Shoten, Tokyo, pp. 199-216.
- McRoy C. P., D. A. Hansell, A. Springer, J. J. Goering, J. J. Walsh and T. E. Whitledge (1987) Global maximum of primary production in the north Bering Sea. *EOS* **68**(50), p. 1727.
- Morgan C. W. and J. M. Bishop (1977) An example of Gulf Stream eddy-induced water exchange in the Mid-Atlantic Bight. *Journal of Physical Oceanography* **7**, 91-99.
- Muller-Karger F. and V. Alexander (1987) Nitrogen dynamics in a marginal sea-ice zone. *Continental Shelf Research* **7**, 805-823.
- Niebauer H. J. and V. Alexander (1985) Oceanographic frontal structure and biological production at an ice edge. *Continental Shelf Research* **4**, 367-388.
- Parsons T. R., Y. Maita and C. M. Lalli (1984) *A manual of chemical and biological methods of seawater analysis*, Pergamon Press, New York, 173 pp.

- Paul J. H. (1983) Uptake of organic nitrogen. In: *Nitrogen in the Marine Environment*, E. J. Carpenter and D. G. Capone, eds., Academic Press, pp. 275-308.
- Price N. M., W. P. Cochlan and P. J. Harrison (1985) Time course of uptake of inorganic and organic nitrogen by phytoplankton in the Strait of Georgia: comparison of frontal and stratified communities. *Marine Ecology-Progress Series* **27**, 39-53.
- Sambrotto R. N., J. J. Goering and C. P. McRoy (1984) Large yearly production of phytoplankton in the western Bering Strait. *Science* **225**, 1147-1150.
- Sambrotto R. N., H. J. Niebauer, J. J. Goering and R. L. Iverson (1986) Relationships among vertical mixing, nitrate uptake and phytoplankton growth during the spring bloom in the southeast Bering Sea. *Continental Shelf Research* **5**, 161-198.
- Selmer J. and F. Sorensson (1986) New procedure for extraction of ammonium from natural waters for ^{15}N isotopic ratio determinations. *Applied and Environmental Microbiology* **52**, 577-579.
- Sharp J. H. (1983) The distribution of inorganic nitrogen and dissolved and particulate organic nitrogen in the sea. In: *Nitrogen in the Marine Environment*, E. J. Carpenter and D. G. Capone, eds., Academic Press, pp. 1-36.
- Smith S. L. and T. E. Whittedge (1977) The role of zooplankton in the regeneration of nitrogen in a coastal upwelling system of northwest Africa. *Deep-Sea Research* **24**, 49-56.
- Springer A. M. (1988) The paradox of pelagic food webs in the northern Bering Sea. Ph.D. Dissertation, University of Alaska Fairbanks, Fairbanks, Alaska, 232 pp.
- Stoker S. (1981) Benthic invertebrate macrofauna of the eastern Bering/Chukchi continental shelf. In: *The Eastern Bering Sea Shelf: Oceanography and Resources*,

- D. W. Hood and J. A. Calder, editors, Univ. Washington Press, Seattle, pp. 1069-1091.
- Sverdrup H. U. (1953) On conditions for the vernal blooming of phytoplankton. *Journal du Conseil, Conseil International pour l'Exploration de la Mer* **18**, 287-295.
- Walsh J. J. (1988) *On the Nature of Continental Shelves*, Academic Press, Inc., 520 pp.
- Walsh J. J., C. P. McRoy, L. K. Coachman, J. J. Goering, J. J. Nihoul, T. E. Whittedge, T. H. Blackburn, P. L. Parker, C. D. Wirick, P. G. Shuert, J. M. Grebmeier, A. M. Springer, R. D. Tripp, D. A. Hansell, S. Djenidi, E. Deleersnijder, K. Henriksen, B. A. Lund, P. Andersen, F. E. Muller-Karger and K. Dean. Carbon and nitrogen cycling within the Bering/Chukchi Seas: source regions for organic matter affecting AOU demands of the Arctic Ocean *Progress in Oceanography* (in press).
- Wheeler P. A. and D. L. Kirchman (1986) Utilization of inorganic and organic nitrogen by bacteria in marine systems. *Limnology and Oceanography* **31**, 998-1009.
- Whittedge T. E., S. C. Malloy, C. J. Patton and C. D. Wirick (1981) Automated nutrient analyses in seawater. Brookhaven National Laboratory Formal Report No. 51398, pp. 227.